Forecasting Rates of Volcanic Activity on Terrestrial Exoplanets

Lynnae C. Quick*
NASA Goddard Space Flight Center
Planetary Geology, Geophysics and Geochemistry Laboratory
8800 Greenbelt Road
Greenbelt, MD
*Corresponding Author: Lynnae.C.Quick@nasa.gov

Aki Roberge
NASA Goddard Space Flight Center
Exoplanets and Stellar Astrophysics Laboratory
8800 Greenbelt Road
Greenbelt, MD

Amy Barr Mlinar
Planetary Science Institute
1700 East Fort Lowell Road
Tucson, AZ 85719

Matthew M. Hedman
University of Idaho
Department of Physics
875 Perimeter Drive
Moscow, ID 83844

Abstract: Similar to the planets and moons in our solar system, terrestrial exoplanets may be shaped by volcanism and tectonics. The magnitudes and rates of geological activity on terrestrial exoplanets will be intimately linked to their sizes and internal heating rates, and can either facilitate, or preclude, the existence of habitable environments. In order to place bounds on the potential for such activity, we estimate total internal heating rates for 52 exoplanets, with masses and radii up to ~ $8M_E$ and $2R_E$, respectively, assuming that internal heating is drawn from both radiogenic and tidal sources. We then compare these internal heating rates to those of the bodies in our solar system in an attempt to constrain the rates of volcanic activity on extrasolar worlds. We find that all of the exoplanets surveyed are likely to exhibit volcanic activity at their surfaces. We also find that at least 25% of the of the planets in our study may be extrasolar ocean worlds, the majority of which may contain internal oceans beneath layers of surface ice. These planets may be similar in structure to the icy moons of the giant planets and may have persistent cryovolcanic activity at their surfaces. Volcanic activity on exoplanets could be detected by next-generation space telescopes in transit spectra. In the case of planets with densities and/or effective temperatures that are consistent with H_2O-rich compositions, spectral identification of excess water vapor and other molecules that are explosively vented into space during cryovolcanic eruptions could serve as a way to infer the presence of subsurface oceans, and therefore indirectly assess their habitability. Considering the implications for habitability, our results suggest that characterizing Earth-like exoplanets in terms of the potential for geological activity at their surfaces should be a priority in the coming years.

1. Introduction

While in some cases volcanism might induce habitable environments on rocky exoplanets [e.g., *Ramirez and Kaltenegger*, 2017], excessive volcanism [*Demory et al.,* 2015] or recurrent, extreme tectonic events (e.g., see [*Hurford et al.*, 2019] would produce unstable surface environments that could render exoplanets incapable of hosing life [*Jackson et al.*, 2008]. The frequency and relative strength of geological activity on rocky extrasolar planets will therefore directly affect their habitability. In order to gauge the habitability of terrestrial exoplanets, it is therefore necessary to constrain the amount of geological activity that may be occurring at their surfaces. Here, we estimate total internal heating rates of 52 terrestrial exoplanets and use these results to constrain rates of volcanic activity at their surfaces, employing rates of volcanic activity on the planets and moons in our solar system as a baseline.

2. Methods

All of the geological activity on the planets and moons in our solar system is driven by internal heating. On Earth, the Moon, and the terrestrial planets, geological processes are driven by radiogenic heating. However on the moons of the giant planets such as Io, Enceladus and Europa, geological processes are primarily driven by tidal heating [*Peale et al.*, 1979; *Cassen et al.*, 1979; *Hurford et al*., 2007; *Meyer and Wisdom*, 2007; *Nimmo et al.*, 2007; *Roberts and Nimmo*, 2008; *Tobie et al.*, 2008]. Terrestrial exoplanets may also experience geological activity as a result of tidal heating from their host stars [*Jackson et al.*, 2008; *Henning and Hurford*, 2014; *Driscoll and Barnes*, 2015; *Barr et al.*, 2018; *Hurford et al.*, 2019; *Makarov et al.*, 2018] as well as due to the decay of radioactive elements in their interiors [*Frank et al.*, 2014]. We therefore assume that geological activity on terrestrial exoplanets is driven by both tidal and radiogenic heating.

If all energy imparted to a planet by tidal dissipation is dispersed as heat as the planet orbits

its parent star, then the amount of heat imparted to the planet by tidal heating can be expressed as:

$$H_{Tidal} = \frac{21}{2}\frac{k_2 \omega^5 {R_P}^5 e^2}{GQ} \quad (1)$$

[*Roberts and Nimmo*, 2008; *Quick and Marsh*, 2015; *Barr et al.*, 2018] where k_2 *i*s the degree 2 love number, which describes how the planet responds to the tide raised on it by its primary. k_2 ranges from 0 for a completely rigid planet, to 1.5 for a planet that is entirely fluid and therefore has a significant tidal response to the gravitational tug of its star. The quantity $\omega \approx \frac{2\pi}{T}$ is the planet's orbital mean motion, with orbital period *T*. R_P represents the planets' radius, and *e* is its eccentricity. Here *G* is the gravitational constant, and *Q* is the quality factor, which represents the fraction of energy that is dissipated as heat within the planet per orbital cycle. *Q* can range from 1 to $1x10^6$ depending on a planet or moon's composition and internal structure [*Goldreich and Soter*, 1966; *Ojakangas and Stevenson*, 1989; *Henning and Hurford*, 2014]. A significant portion of tidal energy is dissipated as heat in the interiors of planets with high *Q*-values.

Frank et al. [2014] provides the radiogenic heating rate, per kg of mantle mass, (henceforth $H^M_{Radiogenic}$) in W/kg, for terrestrial exoplanets as a function of age. Assuming that each planet's mantle makes up 84% of its total mass, as is the case for Earth [*Stacey and Davis*, 2008], the volume of each planet's mantle, V_{Mantle}, can be expressed as:

$$V_{mantle} = 0.84V_P = 0.84 \times \frac{4}{3}\pi R_P^3 \quad (2)$$

If we assume that the density of each exoplanet's mantle, ρ_{Mantle} = 4000 kg/m^3, identical to Earth's mantle, [*Stacey and Davis*, 2008], then the mass of each exoplanet's mantle may be approximated by:

$$M_{mantle} = 0.84 \times \frac{4}{3}\pi R_P^3 \rho_{mantle} \quad (3)$$

Upon obtaining $H^M_{Radiogenic}$ from *Frank et al.* [2014] and assuming that the age of each exoplanet is identical to the average estimated age of its host star, the total radiogenic heating rate for each planet may be expressed as:

$$H_{Radiogenic} = H^M_{Radiogenic} \times M_{mantle} \quad (4)$$

3. Results & Discussion

To demonstrate the utility of (1) and (4) $H_{Radiogenic}$, H_{Tidal}, and H_{Total}, are listed along with physical and orbital parameters, for 52 terrestrial exoplanets in Table 1. We considered planets with $M_P \leq 8\ M_{Earth}$ and $R_P \leq 2R_{Earth}$, which ensures an Earth-like, rather than a sub-Neptune-like, composition [*Stevenson et al.*, 1982; *Borucki et al.*, 2011; *Fabrycky et al.*, 2014]. In addition, we have used the relationship: $H_{Total} = H_{Tidal} + \mathrm{H_{Radiogenic}}$ and assume that the planets don't have substantiative bound atmospheres so that their average surface temperatures, T_S, may be taken to be equal to their effective temperatures, T_{EFF}. We have also substituted $k_2 = 0.3$, consistent with past studies of the terrestrial planets and icy moons in our solar system [*Kozai*, 1968; *Jackson et al*., 2008; *Quick and Marsh*, 2015; *Hurford et al.*, 2019], and $Q = 100$, commensurate with past studies of tidal dissipation in our solar system's moons [e.g., *Peale et al.*, 1979; *Cassen et al.*, 1979; *Chen et al.*, 2014; *Quick and Marsh,* 2015] and the conservative end of studies of tidal dissipation in terrestrial exoplanets [*Henning and Hurford* 2014; *Tamburo et al.*, 2018], into (1). For comparison, Table 1 also includes H_{Total}, $H_{Radiogenic}$ and H_{Tidal}, along with physical parameters for the planets and moons in our solar system. In most cases, internal heating rates and physical

parameters for the bodies in our solar system were extracted from the literature (Table 1 Refs. column). In cases where internal heating rates were not documented in the literature, they were calculated using the formulae introduced above. As is the case for the exoplanets in our study, these calculations assumed that solar system bodies are not fully deformable so that values for H_{Tidal} that are reflective of bodies with homogenous interiors and non-zero rigidities were adopted. (e.g., see Table 3 of *Chen et al.* [2014]). Physical and orbital parameters for each exoplanet were extracted from the NASA Exoplanet Archive and the references listed in Table 1.

We note that with H_{Total} on the order of 10^{14} W (Table 1), Io is the most volcanically active body in our solar system [*Moore*, 2003; *Lopes et al.*, 2004; *McEwen et al.*, 2004]. Further, volcanic and tectonic activity is prevalent on Earth, which has $H_{Total} \sim 4 \times 10^{13}$ W (Table 1) [*Turcotte,* 1995; *Turcotte and Schubert*, 2002], primarily due to radiogenic sources [*Schubert et al.*, 1997; *Turcotte and Schubert*, 2002]. Volcanic and tectonic activity was also widespread on early Venus [*Turcotte*, 1995; *Basilevsky et al.*, 1997; *Schubert et al.*, 1997], which may have had H_{Total} as large as 2×10^{14} W [*Turcotte*, 1995]. Jupiter's icy moon Europa, which has $H_{Total} \sim 1$ TW [*Chen et al.*, 2014; *Quick and Marsh*, 2015], is known to be cryovolcanically and tectonically active [*Fagents*, 2003; *Kattenhorn and Hurford*, 2009; *Prockter and Patterson*, 2009; *Roth et al.*, 2014a; *Sparks et al.*, 2016; 2017; *Prockter et al.*, 2017; *Quick et al.*, 2017b; *Jia et. al.*, 2018], and explosive cryovolcanism, in the form of cold, geyser-like plumes, occurs on both Europa and Saturn's moon Enceladus (Fig. 1) [*Porco et al.*, 2006; *Spencer et al.*, 2009; *Roth et al.*, 2014a; *Sparks et al.* 2016; 2017]. Effusive cryovolcanism, in which slurries of cryogenic fluids quiescently erupt, has been observed on both Europa [*Fagents*, 2003; *Miyamoto et al.*, 2005; *Parro et al.*, 2016; *Prockter et al.*, 2017; *Quick et al.*, 2017b] and Neptune's moon Triton (Fig. 2) [*Croft et al.*, 1995]. We have utilized total internal heating rates, and the associated geological activity on these planets and moons, as a baseline from which the expected rates of volcanic activity on terrestrial exoplanets can be inferred.

3.1 Exoplanet Activity

In the context of this study we first consider 55 Cancri e, which observational analysis has suggested is a highly volcanic lava world that is completely melted on its day side [*Demory et al.,* 2015; 2016], and Corot-7b, which has previously been characterized as a super-Io [*Barnes et al.*, 2010]. Utilizing (1) to calculate the tidal heating rate of 55 Cancri e returns $H_{Tidal} = 4.8 \times 10^{21}$ W (Table 1), while (3) returns $M_{Mantle} = 2.54 \times 10^{25}$ kg. If we assume that each planet's age is identical to the average estimated age of its host star, then the 10.2 Gyr age estimate for 55 Cancri [*von Braun et al.*, 2011] can be utilized to obtain $H^{M}_{Radiogenic} = 4.49 \times 10^{-12}$ W/kg for 55 Cancri e [*Frank et al.*, 2014]. Multiplying this value by M_{Mantle}, as in (4), returns $H_{Radiogenic} = 1.14 \times 10^{14}$ (Table 1). In the case of Corot-7b, (3) returns $M_{Mantle} = 1.4 \times 10^{25}$ kg. We have use the average estimated age of its host star, i.e., 1.32 Gyr [*Barros et al.*, 2014], to obtain $H^{M}_{Radiogenic} = 1.59 \times 10^{-11}$ W/kg [*Frank et al.*, 2014]. Multiplying this value by M_{Mantle} as in (4), returns $H_{Radiogenic} = 2.17 \times 10^{14}$ W for Corot-7b. If $e = 0$ for Corot-7b [*Queloz et al.*, 2009; *Barros et al.*, 2014; *Stassun et al.*, 2017], $H_{Tidal} = 0$ and $H_{Total} = H_{Radiogenic} = 2.17 \times 10^{14}$ W (Table 1). H_{Total} for Io is between 1×10^{14} W and 2×10^{14} W [*Veeder et al.*, 1994; *Spencer et al.*, 2000]. This suggests that 55 Cancri e and Corot-7b are both likely to be very volcanically active. As suggested in previous studies, 55 Cancri e likely exhibits extreme volcanism and may have a molten surface. Identical analyses for L98-59b,c & d [*Kostov et al.*, 2019], assuming that L98-59 and its orbiting planets are at least 1 Gyr old, returns $H_{Radiogenic} = 3.33 \times 10^{13}$ W, 1.6×10^{14} W, and 2.52×10^{14} W, respectively for each planet, with calculated H_{Tidal} and H_{Total} for each world being on the order of 10^{17} W. A simple comparison

of H_{Total} for Io with $H_{Radiogenic}$ for the aforementioned planets (Table 1) makes it clear that even in the absence of tidal heating, 55 Cancri e, Corot-7b, and L98-59 b, c, and d are all likely to exhibit extreme volcanism at their surfaces.

The results for H_{Total} presented in Table 1 can be employed to qualitatively assess the potential for volcanic activity on terrestrial exoplanets compared to the rates at which these processes occur on the planets and moons in our solar system. Owing to their large surface areas through which heat will escape, small planets will have much lower internal temperatures and may cool much faster than large planets [*Stevenson*, 2003]. This will ultimately result in the cessation of geological activity, including volcanism, at their surfaces. In order to constrain the magnitude of volcanic activity occurring on the remainder of the planets in our study, we have plotted H_{Total} as a function of surface area to volume ratio ($SA/V = 3/R$) for the planets and moons in our solar system and 51 terrestrial exoplanets, in Fig. 3. The pink line in Fig. 3 connects Earth, Enceladus, and Europa, all of which are replete with geological activity, including (cryo)volcanism and tectonics. Exoplanets that lie along this line are likely to exhibit similar rates of geological activity as these bodies and may contain internal oceans or magma layers. Exoplanets that lie above this line are likely to display pervasive volcanism and tectonics at their surfaces. Depending on where they plot, rates of volcanism on these exoplanets may be similar to rates of volcanism on Io, Early Venus, or Corot-7b. Rates of volcanism on these bodies may be so high as to be detectable in transit spectra [*Kaltenegger et al.*, 2010; *Quick et al.*, 2017a] or in thermal emission observations [e.g., see *Demory et al.*, 2015].

Planets that lie on or above the blue stippled line are likely to exhibit more subdued geological activity at their surfaces. Similar to the Moon, they may occasionally experience tectonic activity in the form of earthquakes [*Watters et al.*, 2019]. Although widespread volcanism may not occur on these planets, effusive volcanism in the form of (cryo)lava flows may occasionally manifest as it has recently on the Moon [*Garry et al.*, 2012; *Braden et al.*, 2014; *Qiao et al.*, 2017;], Venus [*Smrekar et al.*, 2010] and Jupiter's moon Ganymede [*Head et al.*, 1998; *Schenk et al.*, 2001]. These planets may also experience internal convection on a regional scale similar to Triton [*Schenk and Jackson*, 1993; *Croft et al.*, 1995], and may contain global oceans in their interiors. Pluto, which sits just below the blue stippled line, is known to have internal convection, albeit localized to only a few regions on the surface [*McKinnon et al.*, 2016; *Trowbridge et al.,* 2016], and may also contain a subsurface ocean [*Hammond et al.*, 2016; *Nimmo et al.*, 2016]. It must be noted, however, that the maintenance of an ocean within Pluto may only be possible if the top of the ocean is capped by a layer of insulating clathrates [*Kamata et al.*, 2019]. Consideration of the incorporation of clathrates and other insulating materials into planetary interiors in beyond the scope of this work. However, Pluto's internal state suggests that exoplanets with similar heating rates and surface area to volume ratios might also be able to maintain subsurface liquid reservoirs in special cases where substantial amounts of insulating materials have been incorporated into their interiors. Conversely, exoplanets with lower internal heating rates and significantly larger surface area to volume ratios would plot substantially below the blue stippled line (Fig. 3). These exoplanets would be geologically inactive today. Figure 3 illustrates that the majority of bodies that lie below the blue dotted line have: small radii, on the order of hundreds of km, large surface area to volume ratios, and experience negligible tidal heating. Note that as a result of its large tidal heating rate, H_{Total} for 55 Cancri e is so large that it could not be plotted with the other worlds in Fig. 3.

3.2 Extrasolar Ocean Worlds

Several of the terrestrial planets considered in our study may be more specifically described as ocean planets. Ocean planets are a class of low-density, terrestrial exoplanets with substantial water layers that may be common throughout the galaxy [*Kuchner*, 2003; *Léger et al.*, 2004; *Ehrenreich and Cassan*, 2007; *Sotin et al.*, 2007; *Fu et al.*, 2010]. These planets may exist in one of a variety of climactic states, including, ice-free, partially ice covered, and completely frozen [*Budyko*, 1969; *Sellars*, 1969; *Tajika*, 2008]. In the context of this study, planets that have conditions which are favorable to the maintenance of liquid water on their surfaces or in their interiors are assumed to be ocean planets. Conditions which may be favorable to the maintenance of liquid water include T_{EFF} < 373 K, bulk densities below 5000 kg/m^3 or, in the case of high-gravity planets (Table 1) with potentially high surface pressures (e.g., surface pressures between 10^6 and 10^7 Pa), T_{EFF} below the critical point (i.e., T_{EFF} < 647 K). The effective temperatures (Table 1) and proposed internal structures of Trappist-1c & d [*Barr et al.*, 2018] suggest that they could be ocean planets with surfaces that are covered in liquid water. This could be especially true of Trappist-1d [*Dobos* et al., 2019], as its low density is suggestive of a substantial fraction of volatiles (Table 1). H_{Total} for these planets is 3 x10^{16} W and 3 x 10^{13} W, respectively (Table 1). This indicates that they are likely to have extreme volcanism at their surfaces, with Trappist-1c being more volcanically active than Corot-7b (Fig. 3), in agreement with the results of previous analyses by *Dobos et al.* [2019].

We refer to exoplanets with ice-covered surfaces that overlie internal oceans [*Kuchner*, 2003; *Ehrenreich et al.*, 2006; *Ehrenreich and Cassan*, 2007; Tajika, 2008; *Yang et al.*, 2017] as *cold ocean planets*. The internal structures of cold ocean planets may resemble the internal structures of our solar system's icy moons (Fig. 4) [*Ehrenreich et al.*, 2006; *Sotin et al.*, 2007; *Vance et al.*, 2007; *Fu et al.*, 2010; *Henning and Hurford*, 2014; *Vance et al.*, 2015; *Noack et al.*, 2016; *Luger et al.*, 2017; *Barr et al.*, 2018], and they may exhibit similar geological activity at their surfaces, including ice tectonics [*Fu et al.*, 2010; *Levi et al.*, 2014] and cryovolcanism [*Levi et al.*, 2013; *Quick et al.*, 2017a; *Barr et al.*, 2018; *Quick and Roberge*, 2018]. In the absence of an atmosphere, Earth's effective temperature is 255 K [*Sagan and Mullen*, 1972], which allows for the maintenance of liquid water at the surface. We therefore assume that cold ocean planets have T_{EFF} < 255 K. Several of the planets plotted in Fig. 3 have T_{EFF} < 255 K, and/or densities that are ≤3500 kg/m^3 (Table 1), commensurate with the range of density values for our solar system's icy moons [*Jacobson et al.*, 1992; *Anderson et al.*, 1997; *Hussmann et al.*, 2006]. Based on their surface temperatures and bulk densities, we have designated these exoplanets as cold ocean planets.

The effective temperatures, densities, and total internal heating rates of Kepler 138-b &d, Trappist-1e, f, g & h, Kepler 60-c & d suggest that these planets could be cold ocean planets that have persistent cryovolcanic activity at their surfaces (Table 1 & Fig. 3). Although LHS 1140 b's high-density is indicative of an iron-rich terrestrial planet [*Dittmann et al.*, 2017a; *Ment et al.*, 2019], its 235 K surface temperature [*Ment et al.*, 2019] suggests that any water on its surface would be in a frozen state. Further, its estimated total internal heating rate of almost 2 x 10^{14} W may be high enough for it to maintain an internal ocean and cryovolcanic eruptions at the surface. While cryovolcanic activity on Kepler 138-b and Trappist 1-g & h may be more subdued than what has been observed on Enceladus and Europa (Fig. 1), their plotted positions Fig. 3 suggest that they may undergo periodic resurfacing by cryolava flows and/or experience periodic outgassing of volatiles similar to planet Venus (e.g., see [*Bondarenko et al.*, 2010; *Smrekar et al.*, 2010; *Shalygin et al.*, 2015]). Thus, cryolava flows on the surfaces of these planets may be similar to what has been observed in the walled plains units of Neptune's moon Triton (Fig. 2), albeit more

widespread. Explosive cryovolcanism, similar to what has been observed on Enceladus and Europa (Fig. 1) [*Porco et al.*, 2006; *Spencer et al.*, 2009; *Roth et al.*, 2014a; *Sparks et al.*, 2016; 2017], may occur at comparable magnitudes on Kepler 138d, Trappist-1f and LHS 1140 b.

According to Fig. 3, rates of cryovolcanism on Trappist-1e and Kepler 60 d may be similar to rates of volcanism on Jupiter's moon Io, while Kepler 60c is likely to exhibit extreme cryovolcanism at rates much higher than the silicate volcanism that occurs on Corot-7b. Based on their internal heating rates and surface area to volume ratios compared to the planets and moons in our solar system (Fig. 1), all of the aforementioned exoplanets may contain extensive reservoirs of liquid water, possibly in the form of global oceans beneath layers of surface ice. As is the case for Europa [*Crawford and Stevenson*, 1988; *Fagents*, 2003] and Enceladus [*Manga and Wang*, 2007; *Běhounková et al.*, 2015], cryovolcanic eruptions on these worlds may provide a pathway by which ocean water, or the contents of discrete water pockets within their icy crusts, reaches the surface. It must be noted that in the case of Trappist-1f, g, & h, $H_{Radiogenic}$ is greater than, or equal to, H_{Tidal} (Table 1). Hence, even if Trappist-1f & h are too far away from their host star to experience substantial tidal heating [*Dobos et al.*, 2019], they are still likely to be geologically active and able to maintain subsurface oceans. On the other hand, our analyses suggest that in the absence of tidal heating, Trappist-1g may be geologically dead (see Table 1).

The densities and/or effective temperatures of Trappist-1b, Kepler 93 b, Kepler 138 c, Kepler 114 c, Kepler 80 e, LHS 1140 c, Pi Mensae c, and L 98-59 d are such that they could also be ocean planets or cold ocean planets. If surface pressures on these planets are high enough, liquid water could be maintained at their surfaces at the critical point, or they could contain high pressure ices. These planets are labeled as candidate ocean worlds in Table 1. With the exception of Kepler 114 c, for which we were unable to obtain H_{Total} due to the unknown age of its host star and its unknown eccentricity, estimated internal heating rates for all of these planets suggest that they are all likely to be geologically active (Fig. 3). Of note is that Pi Mensae c and L98-59 d likely receive enough internal heating from radiogenic sources alone to be as volcanically active as Io (Table 1 and Fig. 3), while LHS 1140 c may receive enough internal heating from radiogenic sources alone to be as geologically active as Earth. *Ment et al.* [2019] report an eccentricity less than 0.31 for LHS 1140c. Using 0.31 as an upper bound for eccentricity in (1) results in tidal and total internal heating rates for this planet that are several orders of magnitude greater than the tidal and total internal heating rates for Corot-7 b (Table 1 & Fig 3). Such high internal heating rates would suggest that LHS 1140 c is a lava world instead of a candidate ocean world. However, owing to uncertainties in e [*Ment et al.*, 2019] the estimated H_{Total} for this planet represents a maximum value that may change once e is better constrained. Bearing this mind, we contend that LHS 1140 c may be an ocean world that contains exotic forms of ice on its surface or within its interior. Due to its high T_{EFF} and low density, Pi Mensae c could also contain exotic forms of ice.

3.3 Model Limitations

Utilizing (1) to determine H_{Total} for Io and Enceladus where Jupiter and Saturn serve as the primaries from which tidal heating is sourced, returns total internal heating rates of 2×10^{13} W and $3.2. \times 10^{8}$ W, respectively, which are 1-2 orders of magnitude less than their actual values of 1×10^{14} W, and 1.6×10^{10} W, respectively [*Veeder et al.*, 1994; *Spencer et al.*, 2000; *Schubert et al.*, 2004; *Howett et al.*, 2011]. Enceladus may be considered an outlier as unlike Io where H_{Total} is representative of global heating rates, the bulk of Enceladus' internal heating is concentrated at its south pole [*Howett et al.*, 2011]. Nevertheless, this discrepancy suggests that substituting $k_2 = 0.3$ and $Q = 100$ in (1) returns conservative values for exoplanet tidal heating rates, and by extension,

for the magnitude of geological activity that may be occurring at the surfaces of the exoplanets we have considered. Furthermore, we have not considered additional heating sources that might be contributed by dynamical planet-planet or planet-moon interactions within exoplanetary systems. We have also neglected to consider cases in which the dynamical histories and internal structures of planetary bodies could preclude substantial internal heating. This is the case for Saturn's moon Mimas. Although Mimas is known to be a geologically dead world [*Rhoden et al.* 2017; *Kirchoff et al.*, 2018], utilization of (1) returns a tidal heating rate that suggests that the small moon should be more geologically active than Enceladus. *Neveu and Rhoden* [2019] suggest that the absence of current geological activity on Mimas may be due to a loss of radiogenic heating early in its evolution. These authors assert that loss of radiogenic heating precluded Mimas from having a dissipative interior. Such considerations for Earth-like exoplanets are outside the scope of this work. Nevertheless, the agreement of our results with past studies that considered the magnitude of geological activity on exoplanets (e.g., [*Jackson et al.*, 2008; *Barnes et al.*, 2010; *Demory et al.*, 2015; 2016; *Dobos et al.*, 2019]) illustrates that tidal heating rates obtained using (1), and radiogenic heating rates extracted from *Frank et al.* [2014], can be reliably employed to place conservative estimates on the expected magnitude of internal heating, and by extension, volcanic activity, on solid exoplanets. Our calculations reveal that the majority of exoplanets considered in this study are likely to exhibit volcanic activity, and may also exhibit active tectonics, at levels that are at least on par with, if not greater than, the most geologically active bodies in our solar system. Hence from the standpoint of comparative exoplanetology, in which the internal heating rates and geological activity of the planets and moons in our solar system are used as a baseline, our results regarding the expected magnitude of geological activity on terrestrial exoplanets are robust.

In order to ensure maximum accuracy when constraining the amount of geological activity on the exoplanets listed in Table 1, specific k_2 and Q values must be determined for each planet. This will require a new modeling approach that would allow us to constrain the relative amounts of ice, metal, and rock likely to be present in the planets considered. This approach was investigated in *Barr et al.* [2018] and could be utilized to confirm the terrestrial status of the largest planets in our study, including, Kepler 60c & d, LHS 1140 b, Kepler 138 c, and Pi Mensae c. All of these planets have radii greater than $1.6R_{Earth}$, which could be indicative of a sub-Neptune-like composition [*Rogers et al.*, 2015]. Such an approach will be the focus of a forthcoming manuscript.

4. Conclusions

Based on estimated internal heating rates, all of the exoplanets surveyed here are likely to be geologically active. Comparing calculated internal heating rates of each exoplanet in our study to the estimated internal heating rates of the planets and moons in our solar system indicates that all 52 exoplanets we considered are likely to exhibit moderate to extreme rates of volcanism at their surfaces. In addition, out of the 52 exoplanets that were surveyed, 13 (~ 25%) have effective temperatures and/or densities that are consistent with them being candidate ocean planets. 8 out of these 13 planets (~ 61%) have effective temperatures and/or densities that are indicative of them being cold ocean planets. Hence, about 15% of all of the planets surveyed in this study may be cold ocean planets with internal structures that are similar to the moons of our solar system's giant planets, and similar geological activity at their surfaces. If conditions at the surfaces of candidate ocean planets Trappist-1b, Kepler 93 b, Kepler 138 c, Kepler 114 c, Kepler 80 e, LHS 1140 c, Pi Mensae C and L98-59 d are such that they can maintain liquid water or high-pressure ices, then 21/52 or 40% of the planets surveyed here may be ocean planets. Of note is that these totals do not include cold exoplanets such as OGLE 2005-BLG-390-Lb [*Beaulieu et al.*, 2006], MOA-2007-

BLG-192 [*Bennett et al*., 2008], or OGLE 2016-BLG-1195-Lb [*Shvartzvald et al*., 2017] which were detected by gravitational microlensing. These worlds may be cold ocean planets in their own rights, perhaps containing ice-covered surfaces and internal oceans [*Ehrenreich et* al., 2006; Ehrenreich *and Cassan*, 2007; *Bond et al.*, 2017].

Depending on their total internal heating rates, they could also be geologically active. Our results suggest that a significant number of exoplanets that have been previously classified as terrestrial planets may instead be extrasolar oceans worlds that contain significant amounts of water and may exhibit cryovolcanism and/or ice tectonics at their surfaces. In our solar system, cryovolcanism on the moons of the giant planets serves as an important process that transports liquid water, energy and organics between their interiors and surfaces [*Fagents*, 2003; *Manga and Wang*, 2007; *Lopes et al.*, 2013; *Postberg et al.*, 2018]. In some cases, the circulation of cryomagmatic fluids could create transient habitable niches in the interiors of ice-covered worlds [*Ruiz et al.*, 2007]. Additionally, recent studies suggest that even planets that are mostly ice-covered might have substantial amounts of unfrozen land near their equators where life could flourish [*Paradise et al.*, 2019]. The significant number of candidate cold ocean planets listed in Table 1 suggests that it is important to consider the possibility of habitable environments on terrestrial exoplanets that exist beyond the snowline. Cryovolcanic eruptions on cold ocean planets could be detected by next-generation telescopes as transient or periodic excesses in H_2O, O_2, and/or H in transit spectra that display spatial variability [*Quick et al.*, 2017a], or are localized to one hemisphere, as is the case for the cryovolcanically active moons in our solar system [*Hurford et al.*, 2007; *Hedman et al.*, 2013; *Roth et al.*, 2014a,b; *Rhoden et al.*, 2015; *Sparks et al.*, 2016; 2017; *Teolis et al.*, 2017]. If traces of cryovolcanic activity on exoplanets could be detected in transit spectra, this activity could be used as an indicator of which planets have substantial amounts of internal energy and water, both of which are necessary ingredients for life.

Figure 1. Explosive cryovolcanism, in the form of geyser-like plumes, has been detected on several of the icy moons of the giant planets in our solar system. **(a)** Plumes erupting at the south pole of Saturn's moon Enceladus, as imaged by the Cassini spacecraft. Image Credit: NASA/JPL-Caltech/SSI. **(b)** The Hubble Space Telescope's STIS instrument detected plumes at the south pole of Jupiter's moon Europa. The pixilated blocks represent the locations where water vapor ejected during eruptions was detected spectroscopically. Image Credit: NASA/ESA/L. Roth/SWRI/University of Cologne.

Figure 2. (a) This smooth, semi-circular feature on the surface of Jupiter's moon Europa is believed to be a cryolava flow that was emplaced during an effusive cryovolcanic eruption on the icy moon. (**b)** Cryolava flows on Neptune's moon Triton. Given their densities, effective temperatures, and the estimated magnitude of total internal heating for each, the surfaces of Trappist-1g and Trappist-1h may be covered in cryolava flows.

Figure 3. Based on rates of volcanic activity on Earth, and the rates of cryovolcanic activity on Europa and Enceladus, all bodies on or above the pink line connecting these worlds are likely to have high rates of (cryo)volcanic activity. Worlds on or above the blue dotted line will also be volcanically active, albeit at lower rates. Planetary bodies below the blue dotted line may be geologically dead. Based on this plot, the high rates of internal heating on cold, low-density planets such as Trappist-1h and Kepler 138 b suggest that they are likely to exhibit cryovolcanism similar to what has been observed on Europa and Enceladus. Commensurate with previous investigations, our results suggest that CoRoT-7b's high internal heating rates would induce volcanic activity of a magnitude similar to what has been observed on Jupiter's moon Io.

Figure 4. The internal structures of cold ocean planets may be similar to the internal structures of our solar system's icy moons. The interior structure of Trappist-1h **(a)** [*Barr et al.*, 2018; *Luger et al.*, 2017] may be similar to the interior structure of icy bodies like Jupiter's moon Europa **(b)** [*Schubert et al.*, 2004; 2009].

References

Almenara, J. M., Díaz, R. F., Dorn, C., Bonfils, X., Udry, S., 2018. Monthly Notices of the Royal Astronomical Society 478, 460-486.

Anderson, J. D., Lau, E. L., Sjogren, W. L., Schubert, G., Moore, W. B., 1997. Europa's Differentiated Internal Structure: Inferences from Two Galileo Encounters. Science 276, 1236-1239.

Barnes, R., Raymond, S. N., Greenberg, R., Jackson, B., Kaib, N. A., 2010. CoRoT-7b: Super-Earth or Super-Io? The Astrophysical Journal Letter 709, L95-L98.

Barr, A. C., Dobos, V., Kiss, L. L., 2018. Interior Structures and Tidal Heating in the TRAPPIST-1 Planets. Astronomy and Astrophysics 613, A37.

Barros, S. C. C., Almenar, J. M., Deleuil, M., Diaz, R. F., Csizmadia, Sz., Cabrera, J., Chaintreuil, S., Collier Cameron, A., Hatzes, A., Haywood, R., Lanza, A. F., Aigrain, S., Alonso, R., Bordé, P., Bouchy, F., Deeg, H. J., Erikson, A., Fridlund, M., Grziwa, S., Gandolfi, D., Guillot, T., Guenther, R., Leger, A., Moutou, C., Ollivier, M., Pasternacki, T., Pätzold, M., Rauer, H., Rouan, D., Santerne, A., Schneider, J., Wuchterl, G. 2014. Revisiting the Transits of Corot-7b at a Lower Activity Level. Astronomy and Astrophysics 569, A74.

Basilvesky, A. T., Head, J. W., Schaber, G. G., Strom, R. G., 1997. The Resurfacing History of Venus. In: Bougher, S. W., Hunten, D. M., Phillps, R. J. (Eds.), Venus II. The University of Arizona Press, Tucson, AZ, pp. 1047-1084.

Beaulieu, J. -P., Bennett, D. P., Fouqué, P., Williams, A., Dominik, M., Jørgensen, U. G., Kubas, D., Cassan, A., Coutures, C., Greenhill, J., Hill, K., Menzies, J., Sackett, P. D., Albrow, M., Brillant, S., Caldwell, J. A. R., Calitz, J. J., Cook, K. H., Corrales, E., Desort, M., Dieters, S., Dominis, D., Donatowicz, J., Hoffman, M., Kane, S., Marquette, J.-B., Martin, R., Meintjes, P., Pollard, K., Sahu, K, Vinter, C., Wambsganss, J., Woller, K., Horne, K., Steele, I., Bramich, D. M., Burgdorf, M., Snodgrass, C., Bode, M., Udalski, A., Szymanski, M. K., Kubiak, M., Wieckowski, T., Pietrzynski, G., Soszynski, I., Szewczyk, O., Wyrzykowski, L., Paczynski, B., Abe, F., Bond, I. A., Britton, T. R., Gilmore, A. C., Hearnshaw, J. B., Itow, Y., Kamiya, K., Kilmartin, P. M., Korpela, A. V., Masuda, K., Matsubara, Y., Motomura, M., Muraki, Y., Nakamura, S., Okada, C., Ohnishi, K., Rattenbury, N. J., Sako, T., Sato, S., Sasaki, M., Sekiguchi, T., Sullivan, D. J., Tristram, P. J., Yock, P. C. M., Yoshioka, T., 2006. Discovery of a Cool Planet of 5.5 Earth Masses Through Gravitational Microlensing. Nature 439, 437-440.

Běhounková, M., Tobie, G., Cadek, O., Choblet, G., Porco, C., Nimmo, F., 2015. Timing of Water Plume Eruptions on Enceladus Explained by Interior Viscosity Structure. Nature Geoscience 8, 601-604.

Bennett, D. P., Bond, I. A., Udalski, A., Sumi, T., Abe, F., Fukui, A., Furusawa, K., Hearnshaw, J. B., Holderness, S., Itow, Y., Kamiya, K., Korpela, A. V., Kilmartin, P. M., Lin, W., Ling, C. H., Masuda, K., Matsubara, Y., Miyake, N., Muraki, Y., Nagaya, M., Okumura, T., Ohnishi, K., Perrott, Y. C., Rattenbury, N. J., Sako, T., Saito, T., Sato, S., Skuljan, L., Sullivan, D. J., Sweatman, W. L., Tristram, P. J., Yock, P. C. M., Kubiak, M., Szymanski, M. K., Pietrzynski, G., Soszynski, I., Szewczyk, O., Wyrzykowski, L., Ulaczyk, K., Batista, V., Beaulieu, J. P., Brillant, S., Cassan, A., Fouqué, P., Kervella, P., Kubas, D., Marquette, J. B., 2008. A Low-Mass Planet with a Possible Sub-Stellar-Mass Host in Microlensing Event MOA-2007-BLG-192. The Astrophysical Journal 684, 663-683.

Berger, T. A., Huber, D., Gaidos, E., van Saders, J. L., 2018. Revised Radii of Kepler Stars and Planets Using Gaia Data Release 2. The Astrophysical Journal 866, 99.

Berta-Thompson, Z. K., Irwin, J., Charbonneau, D., Newton, E. R., 2015. A Rocky Planet Transiting a Nearby Low-Mass Star. Nature 527, 204-207.
Bond, I. A., Bennett, D. P., Sumi, T., Udalski, A., et al., 2017. The Lowest Mass Ratio Planetary Microlens: OGLE 2016-BLG-1195 b. Monthly Notices of the Royal Astronomical Society 469, 2434-2440.
Bondarenko, N. V., Head, J. W., Ivanov, M. A., 2010. Present-Day Volcanism on Venus: Evidence from Microwave Radiometry. Geophysical Research Letters 37, L23202.
Bonfils, X., Almenara, J.-M., Cloutier, R., Wünsche, A., et al., 2018. Radial Velocity Follow-Up of GJ1132 with HARPS: A Precise Mass for Planet b and the Discovery of a Second Planet. Astronomy and Astrophysics 618, A142.
Bonomo, A. S., Sozzetti, A., Lovis, C., Malavolta, L., et al., 2014. Characterization of the Planetary System Kepler-101 with HARPS-N: A Hot Super-Neptune with an Earth-Sized Low-Mass Companion. Astronomy and Astrophysics 572, A2.
Borucki, W. J., Koch, D. G., Batalha, N., Bryson, S. T., et al., 2012. Kepler-22b. A 2.4 Earth-Radius Planet in the Habitable Zone of A Sun-Like Star. The Astrophysical Journal 745, 120.
Borucki, W. J., Agol, E., Fressin, F., Kaltenegger, L., et al., 2013. Kepler-62: A Five-Planet System with Planets of 1.4 and 1.6 Earth Radii in the Habitable Zone. Science 340, 587-590.
Braden, S. E., Stopar, J. D., Robinson, M. S., Lawrence, S. J., van der Bogert, C. H., Hiesinger, H., 2014. Evidence for Basaltic Volcanism on the Moon within the Past 100 Million Years. Nature Geoscience 7, 787-791.
Budyko, M. I., 1969. The Effect of Solar Radiation Variations on the Climate of the Earth. Tellus 21, 611-619.
Carter, J. A., Agol, E., Chaplin, W. J., Basu, S., et al., 2012. Kepler-36: A Pair of Planets with Neighboring Orbits and Dissimilar Densities. Science 337, 556-559.
Cassen, P., Reynolds, R. T., Peale, S. J., 1979. Is There Liquid Water on Europa? Geophysical Research Letters 6, 731-734.
Castillo-Rogez, J. C., Hesse, M. A., Formisano, M., Sizemore, H., Bland, M., Ermakov, A. I., Fu, R. R., 2019. Conditions for the Long-Term Preservation of a Deep Brine Reservoir in Ceres. Geophysical Research Letters 46, 1963-1972.
Charpinet, S., Fontaine, G., Brassard, P., Green, E. M., et al., 2011. A Compact System of Small Planets Around a Former Red-Giant Star. Nature 480, 496-499.
Chen, E. M. A., Nimmo, F., Glatzmaier, G. A., 2014. Tidal Heating in Icy Satellite Oceans. Icarus 229, 11-30.
Christiansen, J. L., Vanderburg, A., Burt, J., Fulton, B. J., et al., 2019. Three's Company: An Additional Non-Transiting Super-Earth in the Bright HD 3167 System, and Masses for All Three Planets. The Astronomical Jouranl 154, 122.
Cook, J. C., Desch, S. J., Roush, T. L., Trujillo, C. A., Geballe, T. R., 2007. Near-Infrared Spectroscopy of Charon: Possible Evidence for Cryovolcanism on Kuiper Belt Objects. The Astrophysical Journal 663, 1406-1419.
Crawford, G.D., Stevenson, D.J., 1988. Gas-Driven Water Volcanism and the Resurfacing of Europa. Icarus 73, 66-79.
Croft, S. K., Kargel, J. S., Kirk, R. L., Moore, J. M., Schenk, P. M., Strom, R. G., 1995. The Geology of Triton. In: Cruikshank, D. P. (Ed.), Neptune and Triton. University of Arizona Press, Tucson, AZ, pp. 895-964.
Demory, B.-O., Gillon, M., Deming, D., Valencia, D., Seager, S., Benneke, B., Lovis, C.,

Cubillos, P., Harrington, J., Stevenson, K. B., Mayor, M., Pepe, F., Queloz, D., Ségransan, D., Udry, S., 2011. Detection of a Transit of the Super-Earth 55 Cancri e with Warm Spitzer. Astronomy and Astrophysics 533, A114.

Demory, B.-O., Gillon, M., Madhusudhan, N., 2015. Variability in the Super-Earth 55 Cnc e. Monthly Notices of the Royal Astronomical Society 455, 2018-227.

Demory, B.-O., Gillon, M. de Wit, J., Madhusudhan, N., Bolmont, E., Heng, K., Kataria, T., Lewis, N., Hu, R., Krick, J., Stamenkovic, V., Benneke, B., Kane, S., Queloz, D., 2016. A Map of the Large Day-Night Temperature Gradient of a Super-Earth Exoplanet. Nature 532, 207-222.

Dittmann, J. A., Irwin, J. M., Charbonneau, D., Bonfils, X., 2017a. A Temperate Rocky Super-Earth Transiting a Nearby Cool Star. Nature 544, 333-336.

Dittmann, J. A., Irwin, J. M., Charbonneau, D., Berta-Thompson, Z. K., Newton, E. R., 2017b. A Search for Additional Bodies in the GJ 1132 Planetary System from 21 Ground-Based Transits and a 100-hr Spitzer Campaign. The Astronomical Journal 154, 142.

Dobos, V., Barr, A. C., Kiss, L. L., 2019. Tidal Heating and the Habitability of the Trappist-1 Exoplanets. Astronomy and Astrophysics 624, A2.

Dressing, C. D., Charbonneau, D., Dumusque, X., Gettel, S. 2015. The Mass of Kepler-93b and the Composition of Terrestrial Planets. The Astrophysical Journal 800, 135.

Driscoll, P. E., Barnes, R., 2015. Tidal Heating of Earth-Like Exoplanets Around M Stars: Thermal, Magnetic, and Orbital Evolutions. Astrobiology 15, 739-760.

Ehrenreich, D., Lecavelier des Etangs, A., Beaulieu, J.-P., Grasset, O., 2006. On the Possible Properties of Small and Cold Extrasolar Planets: Is OGLE 2005-BLG-390Lb Entirely Frozen? The Astrophysical Journal 651, 535-543.

Ehrenreich, D., Cassan, A., 2007. Are Extrasolar Oceans Common Throughout the Galaxy? Astronomische Nachrichten 328, 789-792.

Esteves, L. J., De Mooij, E. J. W., Jayawardhana, R., 2015. Changing Phase of Alien Worlds: Probing Atmospheres of Kepler Planets with High-Precision Photometry. The Astrophysical Journal 804, 150.

Everett, M. E., Barclay, T., Ciardi, D. R., Horch, E. P., Howell, S. B., Crepp, J. R., Silva, D. R., 2015. High-Resolution Multi-Band Imagaing for Validation and Characterization of Small Kepler Planets. The Astronomical Journal 149, 55.

Fabrycky, D. C., Lissauer, J. J., Ragozzine, D., Rowe, J. F., Steffen, J. H., Agol, E., Barclay, T., Bathala, N., Borucki, W., Ciardi, D. R., Ford, E. B., Gautier, T. N., Geary, J. C., Holman, M. J., Jenkins, J. M., Li, J., Morehead, R. C., Morris, R. L., Shporer, A., Smith, J. C., Still, M., Van Cleve, J., 2014. Architecture of Kepler's Multi-Transiting Systems. II. New Investigations with Twice as Many Candidates. The Astrophysical Journal 790, 146.

Fagents, S.A., 2003. Considerations for Effusive Cryovolcanism on Europa: The Post Galileo Perspective. Journal of Geophysical Research 108, 5139.

Frank, E. A., Meyer, B. S., Mojzsis, S. J., 2014. A Radiogenic Heating Evolution Model for Cosmochemically Earth-Like Exoplanets (Supplementary Info). Icarus 243, 274-286.

Fu, R., O'Connell, R. J., Sasselov, D. D., 2010. The Interior Dynamics of Water Planets. The Astrophysical Journal 708, 1326-1334.

Gaeman, J., Hier-Majumder, S., Roberts, J. H., 2012. Sustainability of a Subsurface Ocean within Triton's Interior. Icarus 220, 339-347.

Garry, W. B., Robinson, M. S., Zimbelman, J. R., Bleacher, J. E., Hawke, B. R., Crumpler, L. S., Braden, S. E., Sato, H., 2012. The Origin of Ina: Evidence for Inflated Lava Flows on the

Moon. Journal of Geophysical Research 117, E00H31.
Gillon, M., Demory, B.-O., Van Grootel, V., Motalebi F., et al., 2017a.Two Massive Rocky Planets Transiting a K-Dwarf 6.5 Parsecs Away. Nature Astronomy 1, 0056.
Gillon, M., Triaud, A. H. M. J., Demory, B.-O., Jehin, E., Agol, E., Deck, K. M., Lederer, S. M., de Wit, J., Burdanov, A., Ingalls, J. G., Bolmont, E., Leconte, J., Raymond, S. N., Selsis, F., Turbet, M., Barkaoui, K., Burgasser, A., Burleigh, M. R., Carey, S. J., Chaushev, A., Copperwheat, C. M., Delrez, L., Fernandes, C. S., Holdsworthm D. L., Kotze, E. J., Van Grootel, V., Almleaky, Y., Benkhaldoun, Z., Magain, P., Queloz, D., 2017b. Seven Temperate Terrestrial Planets Around the Nearby Ultracool Dwarf State TRAPPIST-1. Nature 542, 456-460.
Goldreich, P., Soter, S., 1966. Q in the Solar System. Icarus 5, 375-389.
Gozdziewski, K., Migazewski, C., Panichi, F., Szuszkiewicz, E., 2016. The Laplace Resonance in the Kepler-60 Planetary System. Monthly Notices of the Royal Astronomical Society 455, L104-108.
Hadden, S., Lithwick, Y., 2014. Densities and Eccentricities of 139 Kepler Planets from Transit Time Variations. The Astrophysical Journal 787, 80.
Hammond, N. P., Barr, A. C., Parmentier, E. M., 2016. Recent Tectonic Activity on Pluto Driven by Phase Changes in the Ice Shell. Geophysical Research Letters 43, 6775-6782.
Head, J. W., Pappalardo, R. T., Kay, J., Collins, G., Prockter, L., Greeley, R., Chapman, C., Carr, M., Belton, M. J. S., and the Galileo Imaging Team, 1998. Cryovolcanism on Ganymede: Evidence in Bright Terrain from Galileo Solid State Imaging Data. 29th Lunar and Planetary Science Conference, Abstract #1666.
Hedman, M. M., Gosmeyer, C. M., Nicholson, P. D., Sotin, C., Brown, R. H., Clark, R. N., Baines, K. H., Buratti, B. J., Showalter, M. R., 2013. An Observed Correlation Between Plume Activity and Tidal Stresses on Enceladus. Nature 500, 182-184.
Henning, W. G., Hurford, T. A., 2014. Tidal Heating in Multi-Layered Terrestrial Exoplanets. The Astrophysical Journal 789, 30.
Howett, C. J. A., Spencer, J. R., Pearl, J., Segura, M., 2011. High Heat Flow from Enceladus' South Polar Region Measured Using 10-600 cm^{-1} Cassini/CIRS Data. Journal of Geophysical Research 116, E03003.
Huang, C. X., Burt, J., Vanderburg, A., Günther, M. N., et al., 2018. TESS Discovery of a Transiting Super-Earth in the pi Mensae System. The Astrophyscial Journal Letters 868, L39.
Hurford, T. A., Helfenstein, P., Hoppa, G.V., Greenberg, R., Bills, B. G., 2007. Eruptions Arising from Tidally Controlled Periodic Openings of Rifts on Enceladus. Nature 447, 292-294.
Hurford, T. A., Henning, W. G., Maguire, R., Lekic, V., Schmerr, N., Panning, M., Bray, V., Manga, M., Kattenhorn, S. A., Quick, L. C., Rhoden, A., 2019. Seismicity of Tidally Active Worlds. Icarus, In Revision.
Hussmann, H., Spohn, T., 2004. Thermal Orbital Evolution of Io and Europa. Icarus 171, 391-410.
Hussmann, H., Sohl, F., Spohn, T., 2006. Subsurface Oceans and Deep Interiors of Medium-Sized Outer Planet Satellites and Large Trans-Neptunian Objects. Icarus 185, 258-273.
Jackson, B., Barnes, R., Greenberg, R., 2008. Tidal Heating of Terrestrial Extrasolar Planets and Implications for their Habitability. Monthly Notices of the Royal Astronomical Society 391, 237-245.
Jacobson, R. A., Campbell, J. K., Taylor, A. H., Synnott, S. P., 1992. The Masses of Uranus and

its Major Satellites from Voyager Tracking Data and Earth-Based Uranian Satellite Data. The Astronomical Journal 103, 2068-2078.
Jia, X., Kivelson, M. G., Khurana, K. K., Kurth, W. S., 2018. Evidence of a Plume on Europa from Galileo Magnetic and Plasma Wave Signatures. Nature Astronomy 2, 459-464.
Jontof-Hutter, D., Ford, E. B., Rowe, J. F., Lissauer, J. J., et al., 2016. Secure Mass Measurements from Transit Timing: 10 Kepler Exoplanets Between 3 and 8 $M_{\oplus}$ with Diverse Densities and Incident Fluxes. The Astrophyscial Journal 820, 39.
Kaltenegger, L., Henning, W. G., Sasselov, D. D., 2010. Detecting Volcanism on Extrasolar Planets. The Astronomical Journal 140, 1370-1380.
Kamata, S., Nimmo, F., Sekine, Y., Kuramoto, K., Noguchi, N., Kimura, J., Tani, A., 2019. Pluto's Ocean is Capped and Insulated by Gas Hydrates. Nature Geoscience 12, 407-410.
Kargel, J. S., 1992. Ammonia-Water Volcanism on Icy Satellites: Phase Relations at 1 Atmosphere. Icarus 100, 556-574.
Kattenhorn, S. A., Hurford, T., 2009. Tectonics of Europa. In: Pappalardo, R. T., McKinnon, W. B., Khurana, K. (Eds.), Europa. University of Arizona Press, Tucson, AZ, pp. 199-236.
Kirchoff, M. R., Bierhaus, E. B., Dones, L., Robbins, S. J., Singer, K. N., Wagner, R. J., Zahnle, K. J., 2018. Cratering Histories in the Saturnian System. In: Schenk, P. M., Clark, R. N., Howett, C. J. A., Verbiscer, A. J., Waite, J. H. (Eds.), Enceladus and the Icy Moons of Saturn. University of Arizona Press, Tucson, AZ, pp. 267-284.
Kostov, V. B., Schlieder, J. E., Barclay, T., Quintana, E. V., Colón, K. D., et al., 2019. The L 98-59 System: Three Transiting, Terrestrial-Size Planets Orbiting a Nearby M Dwarf. The Astronomical Journal 158, 32.
Kozai, Y. 1968. Love's Number of the Earth Derived from Satellite Observations. Bulletin Geodesique 89, 355-357.
Kuchner, M. J., 2003. Volatile-Rich Earth Mass Planets in the Habitable Zone. The Astrophysical Journal. The Astrophysical Journal 596, L105-L108.
Léger, A., Selsis, F., Sotin, C., Guillot, T., Despois, D., Mawet, D., Ollivier, M., Labèque, A., Valette, C., Brachet, F., Chazelas, B., Lammber, H., 2004. A New Family of Planets? "Ocean Planets". Icarus 169, 499-504.
Levi, A., Sasselove, D., Podolak, M., 2013. Volatile Transport Inside Super-Earths by Entrapment In the Water-Ice Matrix. The Astrophysical Journal 769, 29.
Levi, A., Sasselove, D., Podolak, M., 2014. Structure and Dynmaics of Cold Water Super-Earths: The Case of Occluded CH_4 and its Outgassing. The Astrophysical Journal 792, 125.
Livingston, J. H., Crossfield, I. J. M., Petigura, E. A., Gonzales, E. J., et al., 2018. Sixty Validated Planets from K2 Campaigns 5-8. The Astronomical Journal 156, 277.
Luger, R., Sestovic, M., Kruse, E., Grimm, S. L., Demory, B.-O., Agol, E., Bolmont, E., Fabrycky, D., Fernandes, C. S., Van Grootel, V., Burgasser, A., Gillon, M., Ingalls, J. G., Jehin, E., Raymond, S. N., Selsis, F., Triaud, A. H. M. J., Barclay, T., Barentsen, G., Howell, S. B., Delrez, L., de Wit, J., Foreman-Mackey, D., Holdsworth, D. L., Leconte, J., Lederer, S., Turbet, M., Almleaky, Y., Benkhaldoun, Z., Magain, P., Morris, B. M., Heng, K., Queloz, D., 2017. A Seven-Planet Resonant Chain in TRAPPIST-1. Nature Astronomy 1, 0129.
Lopes, R. M. C., Kamp, L. W., Smythe, W. D., Mouginis-Mark, P., Kargel, J., Radebaugh, J., Turtle, E. P., Perry, J., Williams, D. A., Carlson, R. W., Douté, S., and the Galileo NIMS and SSI Teams, 2004. Lava Lakes on Io: Observations of Io's Volcanic Activity from Galileo NIMS During the 2001 Fly-Bys. Icarus 169, 140-174.
Lopes, R. M. C., Kirk, R. L., Mitchell, K. L., LeGall, A., Barnes, J. W., Hayes, A., Kargel, J.,

Wye, L., Radebaugh, J., Stofan, E. R., Janssen, M. A., Neish, C. D., Wall, S. D., Wood, C. A., Lunine, J. I., Malaska, M. J., 2013. Cryovolcanism on Titan: New Results from Cassini RADAR and VIMS. Journal of Geophysical Research: Planets 118, 416-435.

López-Morales, M., Haywood, R. D., Coughlin, J. L., Zeng, L., 2016. Kepler-21 b: A Rocky Planet Around a V = 8.25 mag Star. The Astronomical Journal 152, 204.

Luger, R., Sestovic, M., Kruse, E., Grimm, S. L., Demory, B.-O., Agol, E., Bolmont, E., Fabrycky, D., Fernandes, C. S., Van Grootel, V., Burgasser, A., Gillon, M., Ingalls, J. G., Jehin, E., Raymond, S. N., Selsis, F., Triaud, A. H. M. J., Barclay, T., Barentsen, G., Howell, S. B., Delrez, L., de Wit, J., Foreman-Mackey, D., Holdsworth, D. L., Leconte, J., Lederer, S., Turbet, M., Almleaky, Y., Benkhaldoun, Z., Magain, P., Morris, B. M., Heng, K., Queloz, D., 2017. A Seven-Planet Resonant Chain in TRAPPIST-1. Nature Astronomy 1, 0129.

MacDonald, M. G., Ragozzine, D., Fabrycky, D. C., Ford, E. B., et al., 2016. A Dynamical Analysis of the Kepler-80 System of Five Transiting Planets. The Astronomical Journal 152, 105.

Makarov, V. V., Efroimsky, M., 2014. Tidal Dissipation in a Homogenous Spherical Body II. Three Examples: Mercury, Io, and Kepler-10b. The Astrophysical Journal 795, 7.

Makarov, V. V., Berghea, C. T., Efroimsky, M., 2018. Spin-Orbital Tidal Dynamics and Tidal Heating in the TRAPPSIT-1 Multiplanet System. The Astrophysical Journal 857, 142.

Manga, M., Wang, C.-Y., 2007. Pressurized Oceans and the Eruption of Liquid Water on Europa and Enceladus. Geophysical Research Letters 34, L07202.

Manga, M., Zhai, G., Wang, C.-Y., 2019. Squeezing Marsquakes Out of Groundwater. Geophysical Research Letters 46, 6333-6340.

Marcy, G.W., Isaacson, H., Howard, A. W., Rowe, J. F., et al., 2014. Masses, Radii, and Orbits of Small Kepler Planets: The Transition from Gaseous to Rocky Planets. The Astrophysical Journal Supplement Series 2010, 20.

McEwen, A. S., Keszthelyi, L. P., Lopes, R., Schenk, P. M., Spencer, J. R., 2004. The Lithosphere and Surface of Io. In: Bagenal, F., Dowling, T., McKinnon, W. (Eds.), Jupiter: The Planet, Satellites, and Magnetosphere. Cambridge University Press, New York, NY, pp. 307-328.

McKinnon, W. B., Nimmo, F., Wong, T., Schenk, P. M., White, O. L., Roberts, J. H., Moore, J. M., Spencer, J. R., Howard, A. D., Umurhan, O. M., Stern, S. A., Weaver, H. A., Olkin, C. B., Young, L. A., Smith, K.E., and the New Horizons Geology, Geophysics, and Imaging Theme Team, 2016. Convection in a Volatile Nitrogen-Ice-Rich Layer Drives Pluto's Geological Vigour. Nature 534, 82-85.

Ment, K., Dittmann, J. A., Astudillo-Defru, N., Charbonneau, D. et al., 2019. A Second Terrestrial Planet Orbiting the Nearby M Dwarf LHS 1140. The Astronomical Journal 157, 32.

Meyer, J., Wisdom, J., 2007. Tidal Heating in Enceladus. Icarus 188, 535-539.

Mills, S. M., Howard, A. W., Weiss, L. M., Steffen, J. H., et al., 2019. Long-Period Giant Companions to Three Compact, Multiplanet Systems. The Astronomical Journal 157, 145.

Miyamoto, H., Mitri, G., Showman, A. P., Dohm, J. M., 2005. Putative Ice Flow on Europa: Geometric Patterns and Relation to Topography Collectively Constrain Material Properties And Effusion Rates. Icarus 177, 413-424.

Moore, W. B., 2003. Tidal Heating and Convection in Io. Journal of Geophysical Research 108, 5096.

Moore, W. B., Schubert, G., 2003. The Tidal Response of Ganymede and Callisto with and without Liquid Water Oceans. Icarus 166, 223-226.

Morton, T. D., Bryson, S. T., Coughlin, J. L., Rowe, J. F., Ravichandran, G., Petigura, E. A., Haas,

M. R., Batalha, N. M., 2016. The Astrophysical Journal 882, 86.
Muirhead, P. S., Johnson, J. A., Apps, K., Carter, J. A., Morton, T. D., Fabrycky, D. C., Pineda, J. S., Bottom, M., Rojas-Ayala, B., Schlawin, E., Hamren, K., Covey, K. R., Crepp, J. R., Stassun, K. G., Pepper, J., Hebb, L., Kirby, E. N., Howard, A. W., Isaacson, H. T., Marcy, G. W., Levitan, D., Diaz-Santos, T., Armus, L., Lloyd, J. P., 2012. Characterizing the Cool KOIs. III. KOI 961: A Small Star with Large Proper Motion and Three Small Planets. The Astrophysical Journal 747, 144.
Neveu, M., Rhoden, A. R., 2019. Evolution of Saturn's Mid-Sized Moons. Nature Astronomy 3, 543-552.
Nimmo, F., Spencer, J. R., Pappalardo, R. T., Mullen, M. E., 2007. Shear Heating as the Origin of the Plumes and Heat Flux on Enceladus. Nature 447, 289-291.
Nimmo, F., Hamilton, D. P., McKinnon, W. B., Schenk, P. M., Binzel, R. P., Bierson, C. J., Beyer, R. A., Moore, J. M., Stern, S. A., Weaver, H. A., Olkin, C. B., Young, L. A., Smith, K. E. and New Horizons Geology, Geophysics & Imagining Theme Team, 2016. Reorientation of Sputnik Planitia Implies a Subsurface Ocean on Pluto. Nature 540, 94-96.
Noack, L., Höning, D., Rivoldini, A., Heistracher, C., Zimov, N., Journaux, B., Lammer, H., Van Hoolst, T., Bredehöft, J. H., 2016. Water-Rich Planets: How Habitable is A Water Layer Deeper than on Earth? Icarus 277, 215-236.
Ogawa, M., 2016. Evolution of the Interior of Mercury Influenced by Coupled Magmatism-Mantle Convection System and Heat Flux from Core. Journal of Geophysical Research: Planets 121, 118-136.
Ojakangas, G. W., Stevenson, D. J., 1989. Thermal State of an Ice Shell on Europa. Icarus 81, 220-241.
Paige, D. A., Siegler, M. A., 2016. New Constraints on Lunar Heat Flow Rates from LRO Diviner Lunar Radiometer Experiment Polar Observations. 47th Lunar and Planetary Science Conference, Abstract #2753.
Paradise, A., Menou, K., Valencia, D., Lee, C., 2019. Habitable Snowballs: Temeperate Land Conditions, Liquid water, and Implications for CO_2 Weathering. Journal of Geophysical Research: Planets 124, 1-14.
Parro, L. M., Ruiz, J., Pappalardo, R. T., 2016. Timing of Chaotic Terrain Formation in Argadnel Regio, Europa, and Implications for Geological History. Planetary and Space Science 130, 24-29.
Parro, L. M., Jiménez-Díaz, A., Mansilla, F., Ruiz, J., 2017. Present-Day Heat Flow Model of Mars. Nature 7, 45629.
Peale, S. J., Cassen, P., Reynolds, R. T., 1979. Melting of Io by Tidal Dissipation. Science 203, 892-894.
Pepe, F., Collier Cameron, A., Latham, D. W., Molinari, E., 2013. An Earth-Sized Planet with an Earth-Like Density. Nature 503, 377-380.
Peplowski, P. N., Evans, L. G., Hauck II, S. A., McCoy, T. J. et al., 2011. Radioactive Elements on Mercury's Surface from Messenger: Implications for the Planet's Formation and Evolution.Science 333, 1850-1852.
Porco, C. C., Helfenstein, P., Thomas, P. C., Ingersoll, A. P., Wisdom, J., West, R., Neukum, G., Denk, T., Wagner, R., Roatsch, T., Kieffer, S., Turtle, E., McEwen, A., Johnson, T. V., Rathbun, J., Veverka, J., Wilson, D., Perry, J., Spitale, J., Brahic, A., Burns, J. A., DelGenio, A. D., Dones, L., Murray, C. D., Squyres, S., 2006. Cassini Observes the Active South Pole of Enceladus. Science 311, 1393-1401.

Postberg, F., Khawaja, N., Abel, B., Choblet, G., Glein, C. R., Gudipati, M. S., Henderson, B. L., Hsu, H.-W., Kempf, S., Klenner, F., Moragas-Klostermeyer, G., Magee, B., Nölle, L., Perry, M., Reviol, R., Schmidt, J., Srama, R., Stolz, F., Tobie, G., Trieloff, M., Waite, J. H., 2018. Macromolecular Organic Compounds from the Depths of Enceladus. Nature 558, 564-568.

Prockter, L. M., Patterson, G.W., 2009. Morphology and Evolution of Europa's Ridges and Bands. In: Pappalardo, R. T., McKinnon, W. B., Khurana, K. (Eds.), Europa. University of Arizona Press, Tucson, AZ, pp. 237-258.

Prockter, L. M., Shirley, J. H., Dalton III, J. B., Kamp, L., 2017. Surface Composition of Pull-Apart Bands in Argadnel Regio, Europa: Evidence of Localized Cryovolcanic Resurfacing During Basin Formation. Icarus 285, 27-42.

Qiao, L., Head, J., Wilso, L., Xiao, L., Kreslavsky, M., Dufek, J., 2017. Ina Pit Crater on the Moon: Extrusion of Waning-Stage Lava Lake Magmatic Foam Results in Extremely Young Crater Retention Ages. Geology 45, 455-458.

Queloz, D., Bouchy, F., Moutou, C., Hatzes, A., et al., 2009. The Corot-7 Planetary System: Two Orbiting Super-Earths. Astronomy and Astrophysics 506, 303-319.

Quick, L. C., Marsh, B. D., 2015. Constraining the Thickness of Europa's Water-Ice Shell: Insights from Tidal Dissipation and Conductive Cooling. Icarus 253, 16-24.

Quick, L. C., Adams, E., Barr, A. C., 2017a. Prospects for Detecting Cryovolcanic Activity in Exoplanetary Systems. Planetary Science Vision 2050 Workshop, Abstract #8036.

Quick, L. C., Glaze, L. S., Baloga, S. M., 2017b. Cryovolcanic Emplacement of Domes on Europa. Icarus 284, 477-488.

Quick, L. C., Roberge, A., 2018. The Potential for Volcanism and Tectonics on Extrasolar Terrestrial Planets. 231st Meeting of the American Astronomical Society, Paper # 439.21.

Quintana, E. V., Barclay, T., Raymond, S. N., Rowe, J. F., 2014. An Earth-Sized Planet in the Habitable Zone of a Cool Star. Science 344, 277-280.

Ramirez, R., Kaltenegger, L., 2017. A Volcanic Hydrogen Habitable Zone. The Astrophysical Journal Letters 837: L4.

Rhoden, A. R., Hurford, T. A., Roth, L., Retherford, K., 2015. Linking Europa's Plume Activity to Tides, Tectonics, and Liquid Water. Icarus 253, 169-178.

Rhoden, A. R., Henning, W., Hurford, T. A., Patthoff, D. A., Tajeddine, R., 2017. The Implications of Tides on the Mimas Ocean Hypothesis. Journal of Geophysical Research: Planets 122, 400-410.

Roberts, J. H., Nimmo, F., 2008. Tidal Heating and the Long-Term Stability of a Subsurface Ocean on Enceladus. Icarus 194, 675-689.

Robuchon, G., Nimmo, F., 2011. Thermal Evolution of Pluto and Implications for Surface Tectonics and a Subsurface Ocean. Icarus 216, 426-439.

Rogers, L. A., 2015. Most 1.6 Earth-Radii Planets are Not Rocky. The Astrophysical Journal 801, 41.

Roth, L., Saur, J., Retherford, K.D., Strobel, D.F., Feldman, P.D., McGrath, M.A., Nimmo, F., 2014a. Transient Water Vapor at Europa's South Pole. Science 343, 171-174.

Roth, L., Retherford, K.D., Saur, J., Strobel, D.F., Feldman, P.D., McGrath, M.A., Nimmo, F., 2014b. Orbital Apocenter is Not a Sufficient Condition for HST/STIS Detection of Europa's Water Vapor Aurora. Proceedings of the National Academy of Sciences 111, E5123-E5132.

Ruiz, J., Montoya, L., López, V., Amils, R., 2007. Thermal Diapirism and the Habitability of the

Icy Shell of Europa. Origins of Life and Evolution of Biospheres 37, 287-295.
Sagan, C., Mullen, G., 1972. Earth and Mars: Evolution of Atmospheres and Surface Temperatures. Science 177, 52-56.
Schenk, P., Jackson, M. P. A., 2003. Diapirism on Triton: A Record of Crustal Layering and Instability. Geology 21, 299-302.
Schenk, P. M., McKinnon, W. B., Gwynn, D., Moore, J. M., 2001. Flooding of Ganymede's Bright Terrains by Low-Viscosity Water-Ice Lavas. Nature 410, 57-60.
Schubert, G., Spohn, T., Reynolds, R. T., 1986. Thermal Histories, Compositions, and Internal Structures of the Moons of the Solar System. In: Burns, J., Matthews, M. (Eds.), Sattelites. University of Arizona Press, Tucson, AZ, pp.224-292.
Schubert, G., Solomatov, V. S., Tackley, P. J., Turcotte, D. L., 1997. Mantle Convection and Thermal Evolution of Venus. In: Bougher, S. W., Hunten, D. M., Phillps, R. J. (Eds.), Venus II. The University of Arizona Press, Tucson, AZ, pp. 1245-1287.
Schubert, G., Anderson, J. D., Spohn, T., McKinnon, W. B., 2004. Interior Composition, Structure and Dynamics of the Galilean Satellites. In: Bagenal, F., Dowling, T., McKinnon, W. (Eds.), Jupiter: The Planet, Satellites, and Magnetosphere. Cambridge University Press, New York, NY, pp. 281-306.
Schubert, G., Sohl, F., Hussmann, H., 2009. Interior of Europa. In: Pappalardo, R. T., McKinnon, W. B., Khurana, K. (Eds.), Europa. University of Arizona Press, Tucson, AZ, pp. 353-367.
Sellers, W. D., 1969. A Global Climactic Model Based on the Energy Balance of the Earth-Atmosphere System. Journal of Applied Meteorology 8, 392-400.
Shalygin, E. V., Markiewicz, W. J., Basilevsky, A. T., Titov, D. V., Ignatiev, N. I., Head, J. W., 2015. Active Volcanism on Venus in the Ganiki Chasma Rift Zone. Geophysical Research Letters 42, 4762-4769.
Shvartzvald, Y., Yee, J. C., Novati, S. C., Gould, A., et al., 2017. An Earth-Mass Planet in a 1 AU Orbit Around an Ultracool Dwarf. The Astrophysical Journal Letters 840, L3.
Siegler, M. A., Smrekar, S. E., 2014. Lunar Heat Flow: Regional Prospective of the Apollo Landing Sites. Journal of Geophysical Research: Planets 119, 47-63.
Smrekar, S. E., Stofan, E. R., Mueller, N., Trieman, A., Elkins-Tanton, L., Helbert, J., Piccioni, G., Drossart, P., 2010. Recent Hotspot Volcanism on Venus from VIRTIS Emissivity Data. Science 328, 605-608.
Sotin, C., Grasset, O., Mocquet, A., 2007. Mass-Radius Curve for Extrasolar Earth-Like Planets and Ocean Planets. Icarus 191, 337-351.
Sparks, W. B., Hand, K. P., McGrath, M. A., Bergeron, E., Cracraft, M., Deustua, S. E., 2016. Probing for Evidence of Plumes on Europa with HST/STIS. The Astrophysical Journal 829, 121.
Sparks, W. B., Schmidt, B. E., McGrath, M. A., Hand, K. P., Spencer, J. R., Cracraft, M., Deustua, S. E., 2017. Active Cryovolcanism on Europa? The Astrophysical Journal Letters 839, L18.
Spencer, J. R., Rahtbun, J. A., Travis, L. D., Tamparri, L. K., Barnard, L., Martin, T. Z., McEwen, A. S., 2000. Io's Thermal Emission from the Galileo Photopolarimeter-Radiometer. Science 288, 1198-1201.
Spencer, J. R., Barr, A. C., Esposito, L. W., Helfenstein, P., Ingersoll, A. P., Jaumann, R., McKay, C. P., Nimmo, F., Waite, J. H., 2009. Enceladus: An Active Cryovolcanic Satellite. In: Dougherty, M. K., Esposito, L. W., Krimigis, S. M. (Eds.), Saturn from Cassini-Huygens. Springer, New York, NY, pp. 683-724.
Stacey, F. D., Davis, P. M., 2008. Physics of the Earth. Cambridge University Press, Cambridge,

UK.
Stassun, K. G., Collins, K. A., Gaudi, B. S., 2017. Accurate Empirical Radii and Masses of Planets and their Host Stars with Gaia Parallaxes. The Astronomical Journal 153, 136.
Stevenson, D.J., 1982. Formation of the Giant Planets. Planetary and Space Science 30, 755-764.
Stevenson, D. J., 2003. Styles of Mantle Convection and their Influence on Planetary Evolution. Comptes Rendus Geoscience 335, 99-111.
Tajika, E., 2008. Snowball Planets as a Possible Type of Water-Rich Terrestrial Planet in Extrasolar Planetary Systems. The Astrophysical Journal 680, L53-l56.
Tamburo, P., Mandell, A., Deming, D., Garhart, E., 2018. Confirming Variability in the Secondary Eclipse Depth of the Super-Earth 55 Cancri e. The Astronomical Journal 155, 221.
Teolis, B.D., Perry, M. E., Hansen, C. J., Waite, J. H., Porco, C.C., Spencer, J. R., Howett, J. A., 2017. Enceladus Plume Structure and Time Variability: Comparison of Cassini Observations. Astrobiology 17, 926-940.
Tobie, G., Cadek, O., Sotin, C., 2008. Solid Tidal Friction Above a Liquid Water Reservoir as the Origin of the South Pole Hotspots on Enceladus. Icarus 196, 642-652.
Torres, G., Kipping, D. M., Fressin, F., Caldwell, D. A., 2015. Validation of 12 Small Kepler Transiting Planets in the Habitable Zone. The Astrophysical Journal 800, 99.
Trowbridge, A. J., Melosh, H. J., Steckloff, J. K., Freed, A. M., 2016. Vigorous Convection as the Explanation for Pluto's Polygnal Terrain. Nature 534, 79-81.
Turcotte, D. L., 1995. How Does Venus Lose Heat? Journal of Geophysical Research 100, 16931-16940.
Turcotte, D. L., Schubert, G., 2002. Geodynamics, 2nd Edition. Cambridge University Press, New York, NY.
Vance, S., Harnmeijer, J., Kimura, J., Hussmann, H., Demartin, B., Brown, J. M., 2007. Hydrothermal Systems in Small Ocean Planets. Astrobiology 7, 987-1005.
Vance, S., Barnes, R., Brown, J. M., Bollengier, O., Sotin, C., Choukroun, M., 2015. Interior Structure and Habitability of Super-Europas and Super-Ganymedes. 46th Lunar and Planetary Science Conference, Abstract# 2717.
Veeder, G. J., Matson, D. L., Johnson, T. V., Blaney, D. L., Goguen, J. D., 1994. Io's Heat Flow from Infrared RadiometryL 1983-1993. Journal of Geophysical Research 99, 17095-17162.
von Braun, K., Boyajian, T. S., Ten Brummelaar, T. A., Kane, S. R., van Belle, G. T., Ciardi, D. R., Raymond, S. N., López-Morales, M., McAlister, H. A., Schaefer, G., Ridgway, S. T., Sturmann, L., Sturmann, J., White, R., Turner, N. H., Farrington, C., Goldfinger, P. J., 2011. 55 Cancri: Stellear Astrophysical Parameters, A Planet in the Habitable Zone, and Implications for the Radius of a Transiting Super-Earth. The Astrophysical Journal 740, 49.
Wang, S., Wu, D.-H., Barclay, T., Laughlin, G. P., 2017. Updated Masses for the TRAPPIST-1 Planets. ArXiv e-prints, arXiv:1704.04290.
Watters, T. R., Weber, R. C., Collins, G. C., Howley, I. J., Schmerr, N. C., Johnson, C. L., 2019. Shallow Seismic Activity and Young Thrust Faults on the Moon. Nature Geoscience 12, 411-417.
Williams, J.-P., Paige, D. A., Greenhagen, B. T., Sefton-Nash, E., 2017. The Global Surface Temperatures of the Moon as Measured by the Diviner Lunar Radiometer Experiment. Icarus 283, 300-325.
Xie, J.-W., 2014. Transit Timing Variation of Near-Resonance Planetary Pairs. II. Confirmation

of 30 Planets in 15 Multiple-Planet Systems. The Astrophysical Journal Supplement Series 210, 25.
Yang, J., Ding, F., Ramirez, R. M., Peltier, W. R., Hu, Y., Liu, Y., 2017. Abrupt Climate Transition of Icy Worlds from Snowball to Moist or Runaway Greenhouse. Nature Geoscience 10, 556-560.
Yoder, C. F., Peale, S. J., 1981. The Tides of Io. Icarus 47, 1-35.

Table 1. Solar System and Extrasolar Planetary Parameters

World	R_P (R_E)	M_P (M_E)	ρ (kg/m^3)	g (m/s^2)	T_{EFF}/$T_S$$^+$ (K)	System Age (Gyr)	$H_{Radiogenic}$ (W)	H_{Tidal} (W)	H_{Total} (W)	Type	Refs.
Earth	1	1	5500	9.8	255 (T_{EFF}) 288(T_S)	4.5	4 x 10^{13}	_$^{\#}$	4.7 x 10^{13}	rocky	Turcotte, 1995; Turcotte and Schubert, 2002
Venus	0.82	0.95	5240	8.87	260 K (T_{EFF}) 737 (T_S)	4.5	2.91 x 10^{13}	_	2.91 x 10^{13}	rocky	Turcotte, 1995; Schubert et al. 1997
Early Venus	0.82	0.95	5240	8.87	?	4	2 x 10^{14}	_	2 x 10^{14}	rocky	Turcotte, 1995
Io	0.286	0.015	3528	1.8	110	4.5	3.7 x 10^{11}	1 x 10^{14}	1 x 10^{14}	rocky	Yoder and Peale, 1981; Schubert et al., 2004; Hussmann and Spohn, 2004
Europa	0.245	0.008	3000	1.31	100	4.5	2.1 x 10^{11}	1 x 10^{12}	1.21 x 10^{12}	icy	Schubert et al., 2004; Hussmann and Spohn, 2004; &Chen et al., 2014; Quick and Marsh, 2015
Enceladus	0.0395	1.8 x 10^{-5}	1610	0.11	75	4.5	2.73 x 10^{8}	1.6 x 10^{10}	1.63 x 10^{10}	icy	Howett et al., 2011; &Chen et al., 2014
Triton	0.21	0.00359	2060	0.78	38	4.5	7.12 x 10^{10}	*6.6 x 10^{10}	1.37 x 10^{11}	icy	Gaeman et al., 2012; &Chen et al., 2014 and refs. therein
Callisto	0.378	0.018	1834	1.235	126	4.5	3.2 x 10^{11}	3.3 x 10^{9}	3.2 x 10^{11}	icy	Moore and Schubert, 2003; &Chen et al., 2014 and (1)
Ganymede	0.413	0.025	1942	1.43	117	4.5	4.67 x 10^{11}	1.1 x 10^{10}	4.78 x 10^{11}	icy	Moore and Schubert, 2003; Schubert et al., 2004; &Chen et al., 2014 and (1)
Titan	0.404	0.0225	2575	1.35	94	4.5	4.11 x 10^{11}	8.75 x 10^{10}	4.99 x 10^{11}	icy	&Chen et al, 2014; Schubert et al., 1986; and (1)
Mercury	0.38	0.055	5427	3.7	440	4.5	2.25 x 10^{12}	1.4 x 10^{9}	2.25 x 10^{12}	rocky	Peplowski et al., 2011; Makarov & Efroimsky, 2014; Ogawa, 2016**
Mars	0.533	0.107	3934	3.72	210	4.5	2.74 x 10^{12}	1 x 10^{9}	2.74 x 10^{12}	rocky	Parro et al., 2017; Manga et al., 2019
The Moon	0.273	0.012	3344	1.62	215(equator) 104 (poles)	4.5	3 x 10^{11}	_	3 x 10^{11}	rocky	Siegler and Smrekar, 2014; Paige et al., 2016; Williams et al., 2017

Pluto	0.1868	2.18x 10^{-3}	1854	0.620	44	4.5	5.32 x 10^{10}	_	5 x 10^{10}	icy	Robuchon and Nimmo, 2011; McKinnon et al., 2016
Charon	0.095	2.7 x 10^{-4}	1702	0.288	53	4.5	4.4 x 10^{9}	_	4.4 x 10^{9}	icy	Hussmann et al., 2006; Cook et al., 2007
Ceres	0.074	1.5 x 10^{-4}	2160	0.28	150	4.5	4.5 x 10^{9}	_	4.5 x 10^{9}	ice/rock hybrid	Castillo-Rogez et al., 2019
Miranda	0.037	1.1 x 10^{-5}	1200	0.079	60	4.5	8.5 x 10^{7}	_	8.5 x 10^{7}	icy	&Chen et al., 2014
Ariel	0.091	2.3 x 10^{-4}	1592	0.269	60	4.5	3.6 x 10^{9}	_	3.6 x 10^{9}	icy	&Chen et al., 2014
Rhea	0.12	3.9 x 10^{-4}	1233	0.264	99 (dayside) 53(nightside)	4.5	3.3 x 10^{9}	_	3.3 x 10^{9}	icy	&Chen et al., 2014
Mimas	0.03	6.3 x 10^{-6}	1148	0.064	64	4.5	4 x 10^{7}	2.9 x 10^{8}	3.3 x 10^{8}	icy	&Chen et al., 2014
Dione	0.09	1.8 x 10^{-4}	1480	0.232	87	4.5	2.46 x 10^{9}	_	2.46 x 10^{9}	icy	&Chen et al., 2014
55 Cancri e	1.91	8.08	6400	21.7	1958	10.2	1.14 x 10^{14}	4.28 x 10^{21}	4.28 x 10^{21}	rocky	Demory et al., 2011; 2015; 2016
Corot 7 b	5.7	1.55	7500	23	1756	1.32	2.17 x 10^{14}	0 (e = 0)	2.17 x 10^{14}	rocky	Queloz et al., 2009; Barros et al., 2014; Stassun et al., 2017
GJ 1132 b	1.13	1.66	6300	12.9	529	5	3.66 x 10^{13}	TBD: e unknown	3.66 x 10^{13}	rocky	Berta-Thompson et al., 2015; Bonfils et al., 2018; Dittmann et al., 2017b
HD 219134 b	1.6	4.74	6340	18	1015	11	6.42 x 10^{13}	0 (e = 0)	6.42 x 10^{13}	rocky	Gillon et al., 2017a
HD 219134 c	1.5	4.36	6950	18.7	782	11	5.39 x 10^{13}	2.17 x 10^{16}	2.17 x 10^{16}	rocky	Gillon et al., 2017a
ΠHD 219134 f	1.31	unknown	unknown	unknown	522	11	3.51 x 10^{13}	1.42 x 10^{14}	1.77 x 10^{14}	unknown	Gillon et al., 2017a
HD 3167 b	1.7	5.02	5600	17	1669	7.8	9.49 x 10^{13}	0 (e = 0)	9.49 x 10^{13}	rocky	Christiansen et al., 2017; Livingston et al., 2018
Kepler 10 b	1.45	4.6	8255	21	2130	10.6	4.9 x 10^{13}	TBD: e unknown	4.91 x 10^{13}	rocky	Esteves et al., 2015
Kepler 21 b	1.61	5.09	6720	19	2025	3.03	1.48 x 10^{14}	2.6 x 10^{17}	2.6 x 10^{17}	rocky	López-Morales et al., 2016
Kepler 36 b	1.46	4.45	7810	20	978	6.8	6.6 x 10^{13}	2 x 10^{14}	2.7 x 10^{14}	rocky	Carter et al., 2012
Kepler 60 b	1.68	4.2	4620	14	unknown	5.1	1.3 x 10^{14}	9.4 x 10^{14}	1.1 x 10^{15}	ocean planet	Gozdziewski et al. 2016; Jontoff-Hutter et al., 2016; Morton et al., 2016

Kepler 60 c	1.9	3.85	3060	10.4	unknown	5.1	1.7×10^{14}	3.81×10^{15}	3.98×10^{15}	cold planet	Gozdziewski et al. 2016; Jontoff-Hutter et al., 2016; Morton et al., 2016
Kepler 60 d	1.99	4.16	2910	10.3	unknown	5.1	1.97×10^{14}	3.03×10^{14}	5×10^{14}	cold ocean planet	Gozdziewski et al. 2016; Jontoff-Hutter et al., 2016; Morton et al., 2016
Kepler 62 c	0.54	unknown	unknown	unknown	578	7	3.16×10^{13}	TBD: *e* unknown	3.16×10^{13}	unknown	Borucki et al., 2013
Kepler 68 c	0.96	2.04	unknown	21.7	unknown	6.3	1.94×10^{13}	0 (*e* = 0)	1.94×10^{13}	unknown	Berger et al., 2018. Mills et al., 2019
Kepler 70 b	0.76	0.44	5528	7.5	unknown	unknown	TBD: system age unknown	TBD: *e* unknown	unknown	rocky	Charpinet et al., 2011
Kepler 70 c	0.87	0.66	5521	8.5	unknown	unknown	TBD: system age unknown	TBD: *e* unknown	unknown	rocky	Charpinet et al., 2011
Kepler 78 b	1.1	3.2	unknown	14	2250	0.75	9.57×10^{13}	TBD: *e* unknown	9.57×10^{13}	candidate rocky	Pepe et al., 2013; Stassun et al., 2017
Kepler 80 d	1.53	6.75	7040	28	720	2	1.55×10^{14}	TBD: *e* unknown	1.55×10^{14}	rocky	Muirhead et al., 2012; MacDonald et al., 2016
Kepler 80 e	1.6	4.1	3750	16	628	2	1.8×10^{14}	TBD: *e* unknown	1.8×10^{14}	candidate ocean planet	Muirhead et al., 2012; MacDonald et al., 2016
Kepler 93 b	1.6	3.2	4292	12	1037	6.6	8.74×10^{13}	0 (e = 0)	8.74×10^{13}	candidate ocean planet	Dressing et al., 2015; Stassun et al., 2017
Kepler 97 b	1.5	3.5	5440	16	unknown	8.4	5.66×10^{13}	TBD: *e* unknown	5.66×10^{13}	rocky	Marcy et al., 2014
Kepler 99 b	1.5	6.2	10900	28	unknown	1.5	1.66×10^{14}	TBD: *e* unknown	1.66×10^{14}	rocky	Marcy et al., 2014
Kepler 100 b	1.3	7.3	14250	42.5	unknown	6.5	4.7×10^{13}	TBD: *e* unknown	4.7×10^{13}	rocky	Marcy et al., 2014
Kepler 101 c	1.2	unknown	unknown	unknown	1412	5.9	4.3×10^{13}	0 (e = 0)	4.3×10^{13}	candidate rocky	Bonomo et al., 2014
Kepler 102 d	1.2	3.8	13270	28	unknown	1.4	8.66×10^{13}	TBD: *e* unknown	8.66×10^{13}	rocky	Marcy et al., 2014
Kepler 105 c	1.3	4.6	11200	27.3	997	3.5	6.85×10^{13}	TBD: *e* unknown	6.85×10^{13}	rocky	Everett et al., 2015; Jontof-Hutter et al., 2016; Morton et al., 2016
Kepler 114 c	1.6	2.8	4039	11.3	508	2.7	1.49×10^{14}	TBD: *e* unknown	1.49×10^{14}	candidate ocean planet	Muirhead et al., 2012; Xie, 2014; Morton et al., 2016

Kepler 138 b	0.7	0.19	3020	3.8	unknown	4.7	9×10^{12}	5.33×10^{11}	9.5×10^{12}	cold ocean planet	Morton et al., 2016; Almenara et al., 2018
Kepler 138 c	1.7	5.2	6100	18.3	398	4.7	1.3×10^{14}	3.2×10^{13}	1.6×10^{14}	candidate ocean planet	Muirhead et al., 2012; Morton et al., 2016; Almenara et al., 2018
Kepler 138 d	1.7	1.2	1360	4	335	4.7	1.3×10^{14}	1.5×10^{13}	1.4×10^{14}	ocean planet	Muirhead et al., 2012; Morton et al., 2016; Almenara et al., 2018
Kepler 186 b	1.07	unknown	unknown	unknown	579	4	3.6×10^{13}	TBD: *e* unknown	3.6×10^{13}	unknown	Muirhead et al., 2012; Quintana et al., 2014; Torres et al., 2015
Kepler 186 c	1.25	unknown	unknown	unknown	470	4	5.7×10^{13}	TBD: *e* unknown	5.7×10^{13}	unknown	Muirhead et al., 2012; Quintana et al., 2014; Torres et al., 2015
Kepler 186 d	1.4	unknown	unknown	unknown	384	4	8×10^{13}	TBD: *e* unknown	8×10^{13}	unknown	Muirhead et al., 2012; Quintana et al., 2014; Torres et al., 2015
Kepler 186 e	1.27	unknown	unknown	unknown	unknown	4	6×10^{13}	TBD: *e* unknown	6×10^{13}	unknown	Quintana et al., 2014; Torres et al., 2015
Kepler 186 f	1.2	unknown	unknown	unknown	unknown	4	4.7×10^{13}	1.1×10^{9}	4.7×10^{13}	unknown	Torres et al., 2015
Kepler 406 b	1.4	6.4	11820	30	unknown	5.8	6.8×10^{13}	TBD: *e* unknown	6.8×10^{13}	rocky	Marcy et al., 2014
Kepler 406 c	0.85	2.7	24390	37	unknown	5.8	1.4×10^{13}	TBD: *e* unknown	1.4×10^{13}	rocky	Marcy et al., 2014
Kepler 414 b	1.7	3.5	3845	11.7	unknown	5.5	1.14×10^{14}	TBD: *e* unknown	1.14×10^{14}	ocean planet	Hadden and Lithwick, 2014; Morton et al., 2016
L 98-59 b	0.8	0.5	5365	7.6	unknown	1+	3.33×10^{13}	5.72×10^{17}	5.72×10^{17}	rocky	Kostov et al., 2019
L 98-59 c	1.35	2.4	5358	12.9	unknown	1+	1.6×10^{14}	5.38×10^{17}	5.38×10^{17}	rocky	Kostov et al., 2019
L 98-59 d	1.57	3.4	4826	13.5	unknown	1+	2.52×10^{14}	1.68×10^{17}	1.69×10^{17}	candidate ocean planet	Kostov et al., 2019
LHS 1140 b	1.73	6.98	7500	23	235	5^	1.31×10^{14}	[a]6.15×10^{13}	1.93×10^{14}	cold ocean planet	Ment et al., 2019
LHS 1140 c	1.3	1.81	4700	10.8	438	5^	5.34×10^{13}	[a]4.38×10^{18}	4.38×10^{18}	candidate ocean planet	Ment et al., 2019
Pi Mensae c	2.04	4.82	2970	11.3	1169.8	2.98	3×10^{14}	0 (e = 0)	3×10^{14}	rocky	Huang et al., 2018
Trappist-1 b	1.07	0.85	3400	7.3	400	8	2.3×10^{13}	7.02×10^{17}	7.02×10^{17}	candidate	Gillon et al., 2017b;

										ocean planet	Wang et al., 2017
Trappist-1 c	1.04	1.38	7630	12.6	342	8	2.12 x 10^{13}	3.13 x 10^{16}	3.13 x 10^{16}	ocean planet	Wang et al., 2017
Trappist-1 d	0.76	0.41	3950	7	288	8	8.29 x 10^{12}	2.3 x 10^{13}	3.13 x 10^{13}	ocean planet	Gillon et al., 2017b; Wang et al., 2017
Trappist-1 e	0.9	0.64	1710	7.7	251	8	1.39 x 10^{13}	3.84 x 10^{13}	5.23 x 10^{13}	cold ocean planet	Gillon et al., 2017b; Wang et al., 2017
Trappist-1 f	1.03	0.67	1740	6.2	219	8	2.05 x 10^{13}	2.31 x 10^{13}	4.36 x 10^{13}	cold ocean planet	Gillon et al., 2017b; Wang et al., 2017
Trappist-1 g	1.11	1.34	2180	10.7	199	8	2.57 x 10^{13}	5.77 x 10^{11}	2.63 x 10^{13}	cold ocean planet	Wang et al., 2017
Trappist-1 h	0.72	0.086	1270	1.6	167	8	6.99 x 10^{12}	3.03 x 10^{12}	1 x 10^{13}	cold ocean planet	Wang et al., 2017

In the case of non-transiting planets, detected solely by the radial velocity technique, where only planet mass in terms of m sin i is known, we have assumed that planet mass, M_P, is equal to the minimum mass. Planet density, ρ, has been calculated for planets with an unknown bulk density using the relation: $\rho = {3M_P}/{4\pi R_P^3}$. Similarly, surface gravity, g, has been calculated for planets for which surface gravity is unknown using $g = {GM_P}/{R_P^2}$

†T_S corresponds to the mean surface temperature of the planets and moons in our solar system.

#Negligible tidal heating rate

*H_{Tidal} for Triton corresponds to obliquity tides in the subsurface ocean, which contribute more internal energy than solid body tides. See *Chen et al.* [2014].

**$H_{Radiogenic}$ for Mercury calculated using internal heating rate from *Peplowski et al.* [2011] and mantle mass from *Ogawa et al.* [2016]

&We have assumed that moons do not have a fully deformable interior (i.e., $k_2 \neq 1.5$)

∏Smallest possible value of R_p from *Gillon et al.* [2017]

+Minimum stellar age from Kostov et al., 2019

^Minimum stellar age from Ment et al., 2019

[a]Eccentricity is poorly constrained; maximum eccentricity values substituted into (1). H_{Tidal} values are preliminary.

Figure 1

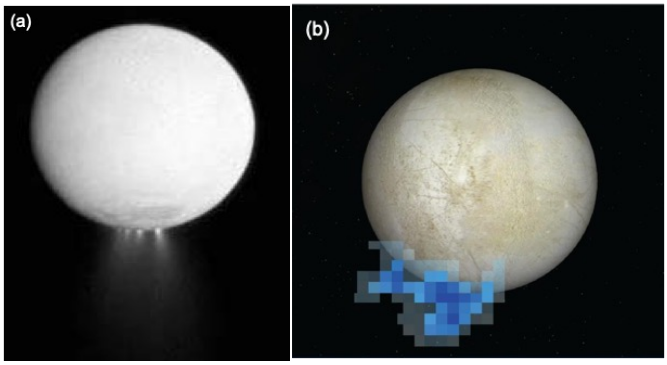

Figure 2

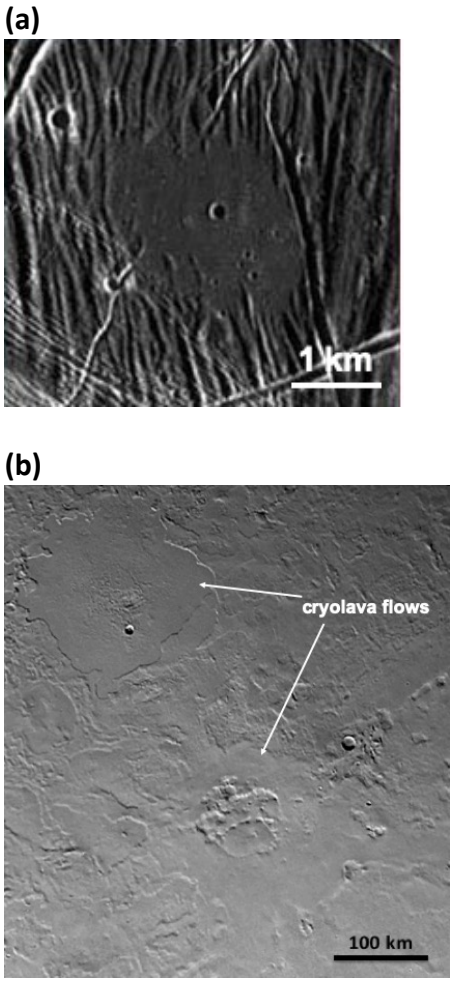

Figure 3

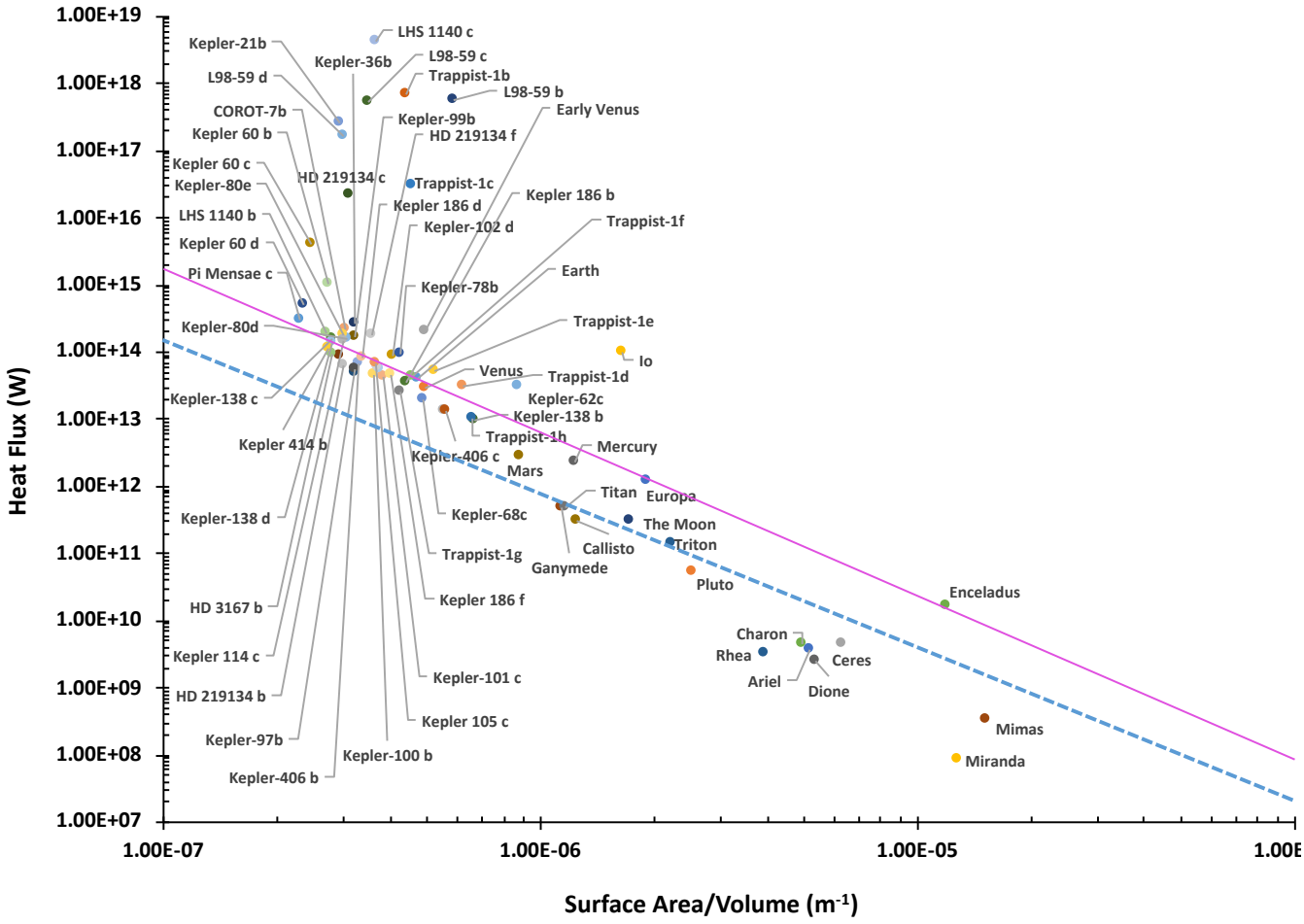
Heat Flux (W)
1.00E+19
1.00E+18
1.00E+17
1.00E+16
1.00E+15
1.00E+14
1.00E+13
1.00E+12
1.00E+11
1.00E+10
1.00E+09
1.00E+08
1.00E+07
1.00E-07
1.00E-06
1.00E-05
1.00E
Surface Area/Volume (m-1)
LHS 1140 c
Kepler-21b
Kepler-36b
L98-59 c
L98-59 d
Trappist-1b
L98-59 b
Early Venus
COROT-7b
Kepler-99b
HD 219134 f
Kepler 60 b
Kepler 60 c
HD 219134 c
Trappist-1c
Kepler-80e
Kepler 186 b
Kepler 186 d
Trappist-1f
LHS 1140 b
Kepler-102 d
Kepler 60 d
Earth
Pi Mensae c
Kepler-78b
Trappist-1e
Kepler-80d
Io
Venus
Trappist-1d
Kepler-138 c
Kepler-62c
Kepler-138 b
Trappist-1h
Kepler 414 b
Mercury
Kepler-406 c
Mars
Titan
Europa
Kepler-138 d
Kepler-68c
The Moon
Triton
Callisto
Trappist-1g
Ganymede
Pluto
Enceladus
HD 3167 b
Kepler 186 f
Charon
Rhea
Ceres
Kepler 114 c
Ariel
Dione
Kepler-101 c
HD 219134 b
Mimas
Kepler 105 c
Kepler-97b
Kepler-100 b
Miranda
Kepler-406 b

Figure 4

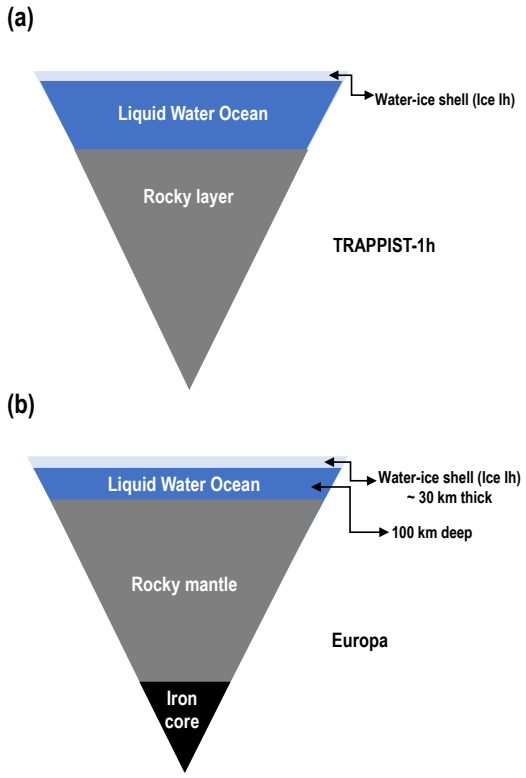
(a)
Liquid Water Ocean
Water-ice shell (Ice Ih)
Rocky layer
TRAPPIST-1h
(b)
Liquid Water Ocean
Water-ice shell (Ice Ih)
~ 30 km thick
100 km deep
Rocky mantle
Europa
Iron core